TMT

ALTERNATE SITE:

OBSERVATORIO DEL ROQUE DE LOS MUCHACHOS

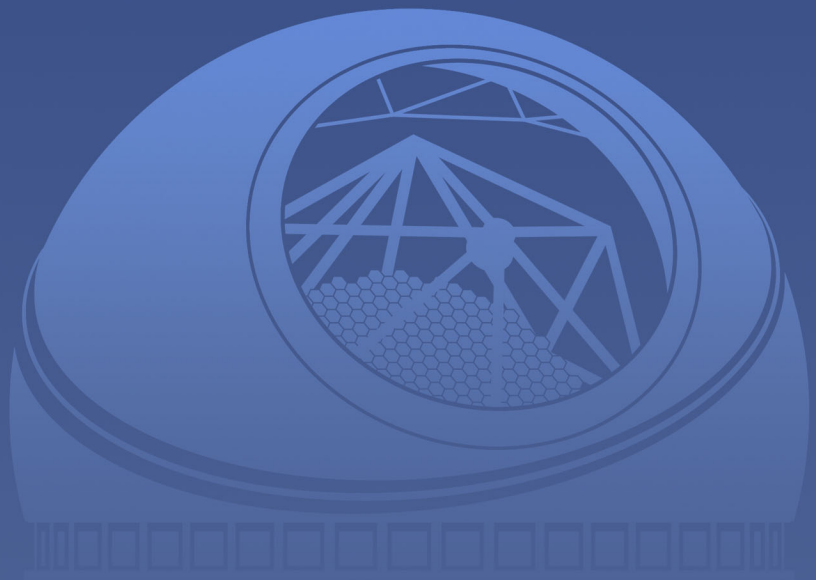

TMT.SIT.TEC.16.083.REL01

July 2021

www.tmt.org

TABLE OF CONTENT

EXECUTIVE SUMMARY

From February 2016 through October 2016, six potential sites (in Chile, China, India, Mexico and Spain) were evaluated for TMT, to provide an alternative location for the observatory in case access to Maunakea would not be possible in a timely way. The site evaluation process covered multiple aspects that included (i) the astronomical properties of the sites for carrying out the TMT science mission, (ii) the legal arrangements for TIO to operate in the host country, (iii) processes and timescales for obtaining necessary permits, (iv) the schedule for initiation of construction, (v) logistical issues for siting the observatory and transporting materials to the site, (vi) the cost to construct and operate TMT at the site, and (vii) an evaluation of the risks to schedule and cost. The astronomical properties of all alternate sites considered were evaluated using the same methodology as for the original 2008 site study, but this time included also data obtained by different groups.

Important findings were that all potential sites considered were excellent sites for carrying out the core science of TMT. Also, the interactions with all host countries and organizations were uniformly very positive and constructive.

In October 2016, the TIO Board of Directors selected the 'Observatorio del Roque de Los Muchachos' (ORM), on La Palma, in the Canary Islands (Spain) as the official alternate site for TMT. This decision was based on (i) the scientific importance for TMT to remain located in the Northern Hemisphere, positioning itself as a facility providing a unique access to the Northern sky, (ii) the fact that TMT core-science could be successfully achieved at ORM, and (iii) the range of benefits provided by ORM (low project risk, improved construction/operations cost & shorter schedule). In this report, we present the results of studies carried out by the TMT Project for describing the conditions of TMT's alternate site. In particular, ORM's characteristics for supporting TMT science programs are compared with those at TMT's baseline site (Maunakea 13N, aka MK13N), but also with Armazones, Chile, which is the site that will host the 39m European ELT.

TMT core science being based on a heavy usage of high-performance adaptive optics (AO) systems, we extensively studied the characteristics of the turbulence profile over all TMT sites. Our study showed that the turbulence profile above ORM is similar in behavior to MK13N, and only second regarding AO performances among all five sites considered (Hawaii and the four alternate site candidates). Using the ORM turbulence profile with our own performance model for TMT's AO facility, we could demonstrate that TMT will perform excellently in its diffraction-limited regime at ORM.

Differences in precipitable water vapor, mean temperature and extinction are in line with expectations based on the sites' altitudes. Extinction and dust characteristics were a major focus during our site evaluation and after examining significant datasets and years of operational experiences by observatories at both Northern sites, these parameters were not found to be discriminating factors. For instance: both Northern sites, MK13N and ORM, have equivalent dust

levels that are lower than the Chilean sites for times when observations are conducted, the number of usable nights is the same, and the extinction statistics for usable nights - regardless of the cause of the extinction - are also equivalent. In the 2016 study we compared the results of mirror reflectivity experimental campaigns and cleaning operation procedures for various telescopes and concluded that mirror reflectivity proceeds at the same rate at all sites evaluated.

The potential impact on scientific productivity between MK13N and ORM can be mainly summarized in terms of science operations efficiency. The vast majority of TMT science goals and science programs can be carried out from either site. Conducting the full range of science observations from ORM would require, on average, to increase the observing time by about 16–19% for the First-Light instruments (WFOS, IRIS, and MODHIS) and future instruments, some observing modes and wavelength ranges being more affected than others.

1. TMT SITE SELECTIONS

TMT's site selection process is arguably one of the most thorough and detailed ever conducted for characterizing and down-selecting the construction site of a ground-based astronomical facility (Schoeck et al., 2009). The original work took place between 2004 and 2008 and included various sites in Chile, one in Mexico (Baja California) and another in the USA (Hawaii), and was preceded by several years of preparatory work, most notably by the study of an extensive series of satellite data measuring cloud coverage and precipitable water vapor (PWV), (see Carrasco et al., 2017 for details of that preliminary work). In July 2009, based on this extensive site evaluation, the TMT Board of Directors selected the "13 North" (13 N) site on Maunakea, Hawaii, (hereafter simply referred to as "MK13N") as the baseline site for the construction of TMT.

As early as 2016, the need to investigate additional alternate sites for TMT was motivated for the following reasons:

(i) a fraction of the native Hawaiian population opposed the project and prevented access to the summit of Maunakea at multiple dates in 2014 and 2015, and

(ii) in December 2015, the Hawaii Supreme Court ruled that the State's permitting process was flawed, and the State Board of Land and Natural Resources was ordered to re-do the permit process.

While a process was engaged to have the permit re-issued in Hawaii, the TMT International Board of Directors made the decision that a study to identify and select an alternate construction site had to be carried out.Table 1 below lists the main sites that were originally considered in this study. The leading organizations for all four candidate alternate sites provided rapid and extensive responses to our requests for information. All expressed their great enthusiasm to host TMT, and their willingness to support all processes to prepare its construction.

The core of TMT science is expected to be produced mainly at visible and near-infrared wavelengths, with a smaller amount of observing time dedicated to mid-infrared observations (roughly 30-40% in the visible, 50-60% in the near-infrared, no more than 10% in the mid-IR). In addition, the strength of telescopes the size on an ELT resides not only within their light-collecting capacity but also within the increase of spatial resolution. The combination of adaptive optics with the 30m extremely large aperture of TMT is most important for delivering the spatial resolution needed by TMT science programs. As a result, in addition to the fraction of usable-nights, or the median uncorrected seeing, other parameters relevant to adaptive optics performance, such as atmospheric coherence time and isoplanatic angle, are paramount for selecting the best TMT alternate site.

Additional considerations for the alternative site investigations were related to site logistics, schedule and uncertainties for obtaining permits, cost of construction and operation, as well as the ability to make a fast start on construction for the case that Maunakea becomes infeasible. The strategic advantages of having a Northern Hemisphere site and unique complementarity to the two others ELT projects were also considered.

It is important to note that all sites listed are excellent sites for astronomy and would enable TMT core-science programs.

Table 1*:* Table of latitude, longitude and altitude for all alternate sites originally considered in our study, including the baseline site MK13N. Armazones, the site of the European ELT (E-ELT), is also included for comparison.

Sites	Altitude	Latitude	Longitude	Comments
Maunakea, (MK13N), USA **(baseline TMT site)**	4050m	19.82°	155.5°W	Data from TMT site-testing
Observatorio Roque de los Muchachos (ORM), Spain	2250m	28.80°	17.9°W	Data from IAC, ESO site-testing groups and ORM telescopes in operations
San Pedro Mártir (SPM), Mexico	2790m	30.75°	115.5°W	TMT site-testing data on Cerro Pelado (2km away)
Cerro Vicuña Mackenna, Chile	3114m	-24.59°	70.0°W	TMT site-testing data on Cerro Armazones (25km away)
Hanle, India	4500m	32.78°	79.0°E	Several short/medium time-span site studies available (India Astronomical Observatory).
Ali, China	5100m	32.31°	80.0°E	Several short/medium time-span site studies available.
Cerro Honar, Chile	5400m	-23.07°	67.8°W	TMT site-testing data on Cerro Tolonchar (100km away) and ALMA site-testing data
Armazones, Chile (E-ELT)	3064 m	24.58° S	70.2° W	Data from TMT site-testing, now the site for the E-ELT

1.1. ORM BECOMES TMT ALTERNATE SITE

After several months of study, the TMT Board of Directors and its Science Advisory Committee agreed that the site of TMT construction should remain in the Northern Hemisphere and, on October 31st, 2016, the TIO Board of Directors selected the 'Observatorio del Roque de Los Muchachos' (ORM), on La Palma, in the Canary Islands (Spain) as the alternate site for TMT. This decision was based on:

- The scientific importance for TMT to be located in the Northern Hemisphere and position itself as a unique facility:
  - A Northern Hemisphere location will secure full sky coverage to the worldwide astronomy community in combination with the two other ELT projects, both to be located in the Southern Hemisphere.
  - The very good quality of the ORM site, which can support all of TMT core science programs and provides AO performances similar to Maunakea.
- The range of benefits provided by the ORM site, including:
  - Reduced construction schedule, lower site-related construction cost, and simplified construction logistics, due to the lower altitude of the site.

- Lower cost and simplified operations due to the availability of existing infrastructure and lower altitude of the site.
- Lower overall project risks due to existence of support infrastructure.

1.1.1. ORM: SITE DESCRIPTION

The ORM site is located on the island of La Palma, in the Northwest of the Canary Islands archipelago. The observatory, which is part of the European Northern Observatory, was inaugurated in 1985 and is currently hosting more than a dozen telescopes and experiments under international leadership (
Figure *1*). The facilities in operations at ORM cover instrumentation functioning over a large domain of wavebands, from gamma-rays to microwaves, and include the 10.4m GranTeCan, the largest optical-infrared telescope worldwide, the first large telescope (23m diameter) of the future Cherenkov Telescope Array North (ultimately composed of 15 medium size (12m) and 4 large size (23m) telescopes) and, citing only some of the main facilities, the 4.2m William Hershel Telescope, the 3.6m Telescopio Nazionale Galileo, the 2.6m Northern Optical Telescope, the 2.5m Isaac Newton Telescope, the 1m Swedish Solar telescope, etc.

The ORM domain covers an area close to 200 hectares and is located on the Northwestern slope of a large volcanic crater, the Calbura de Taburiente National Park. The quality of the sky above La Palma is protected by law since 1988 to control and reduce the light pollution from neighboring cities and the island of Tenerife. The sky above La Palma is also a no-flight zone for commercial aircraft.

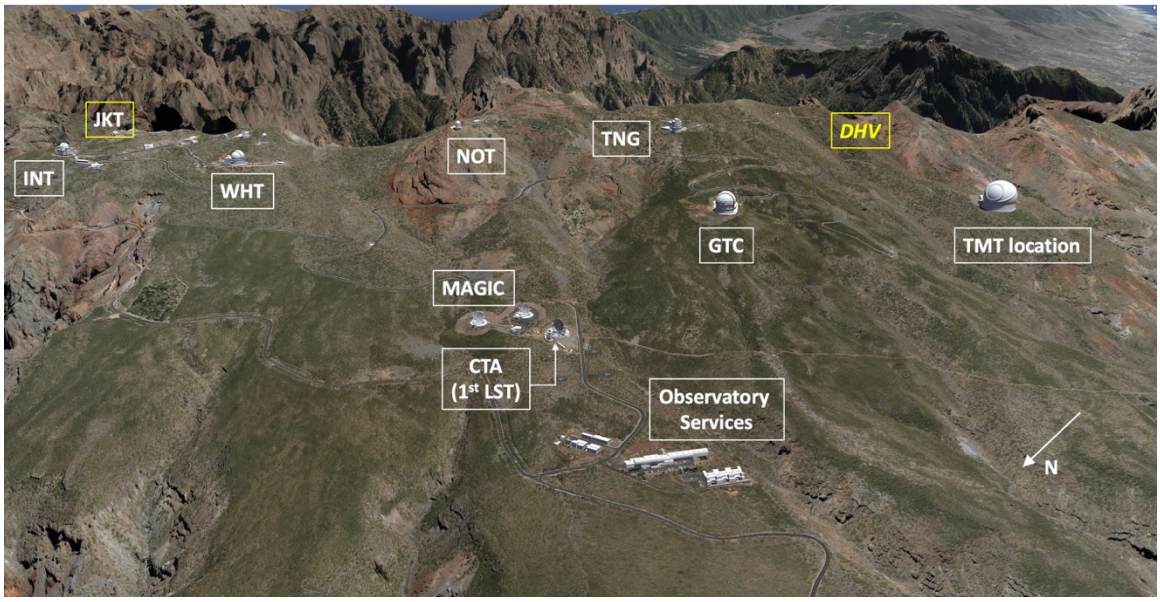

Figure 1: Aerial view of the Observatorio del Roque de los Muchachos (ORM), in La Palma, Canary Islands. The locations of the main telescopes in operations are shown, including the selected location for TMT. We also show the locations where the site-testing data discussed in

this document have been obtained: JKT for the g-SCIDAR data, and DHV (Degollada del Hoyo Verde) for the ESO/E-ELT data.

The conditions above ORM have been extensively studied for more than 20 years (see references in Section 4), including extended DIMM, MASS-DIMM, g-SCIDAR and radiosonde balloon campaigns to determine the atmospheric turbulence profiles. For the TMT study, and to best characterize the turbulence profile, we have elected to analyze the g-SCIDAR data obtained from 2004-2009 at the Jacobus-Kapteyn-Telescope (JKT) site. This data set was the most extensive in duration while providing high-vertical resolution to characterize the strength of the turbulence and its distribution between free-atmosphere and ground-layers. As the JKT site is located on the east side of the observatory, closer to the ridge of the caldera than TMT, we also compared the results of our analysis with ESO's E-ELT campaign results obtained at a location closer to TMT.

Table 2 below lists the main site characteristics of the two Northern sites considered for TMT: MK13N in Hawaii, USA (the baseline site), and ORM in the Canary Islands, Spain (the alternate site). The characteristics of the E-ELT site (Armazones, Chile) are also included for comparison. Also, please note that the visual extinction value reported for Armazones comes from measurements made at Paranal (Patat F., et al., 2011, A&A, 527, A91).

Table 2: Main site characteristics for the two Northern TMT sites MK13N and ORM. The data for the E-ELT are also included for comparison. The estimated fractions of usable time take into account all operational possible losses due to adverse weather conditions.

Site Characteristics (median values, unless stated)	**MK13N (USA)**	**ORM (Spain)**	**Armazones (Chile)**
Altitude of site (m)	4050	2250	3060
Fraction of yearly usable time (%)	72	72	86
Seeing at 60m above ground (arcsecond)	0.50	0.58	0.50
Isoplanatic angle (arcsecond)	2.55	2.31	2.05
Atmospheric coherence time (ms)	7.3	6.0	5.0
Calculated Adaptive Optics Strehl merit function	1.0	0.93	0.92
Precipitable water vapor (% time < 2mm)	54	20	50
Mean nighttime temperature (°C)	2.3	7.6	7.5
Atmospheric Extinction (V_{mag}/airmass)	0.11	0.13	0.13

Table 3 lists the main sources of the measurements used in this study. The data to characterize MK13N and Armazones come from the original and extensive TMT site testing campaign (Schoeck et al., 2009). For the ORM site, we used data, kindly provided to the TMT team by the Site Testing & Sky Quality Team of the Instituto de Astrofísica de Canarias (IAC), and also the European Southern Observatory (ESO), in the context of studies done for the E-ELT project. Some complementary data were obtained directly from the operations teams of the telescopes, such as the Liverpool Robotic Telescope, or the GranTeCan (GTC) telescope for instance.

Table 3: List of the main sources of data used for characterizing the two TMT Northern sites.

Parameter	Data source/method/extent	
	MK13N	ORM
60m seeing and Isoplanatic angle	SODAR and MASS (2 years)	SCIDAR (5.5 years), MASS (200 days)
Atmospheric coherence time	MASS (2 years)	NOAA 200mb winds (20 years), MASS, SCIDAR
Precipitable Water Vapor	IRMA (2 years)	Radiosonde soundings (2 years) and IAC GPS (1 year)
Mean night temperature	Automated Weather Station (2 years)	IAC and NOT group measurements (4.9 years)
Extinction	CFHT Skyprobe (6.8 years)	Carlsberg Meridian Telescope (CMT) extinction measurements (25.4 years)
Dust	On site TMT site testing measurements (2 years)	Telescopio Nazionale Galileo measurements (14.4 years)
Usable time fraction	ASCA, long term satellite studies, operational experiences (2 years)	CMT (25.4 years), Liverpool Robotic Telescope logs (9.5 years), operational experiences

1.1.2. ORM vs MK13N: Seasonal variation of main parameters

In the figures below, [**Figure 2, Figure 3, Figure 4, Figure 5**] we represent the ORM and MK13N seasonal variation of some of the main parameters characterizing the site conditions. The median and interquartile range are plotted for nighttime temperature, seeing, Precipitable Water Vapor (PWV) and windspeed.

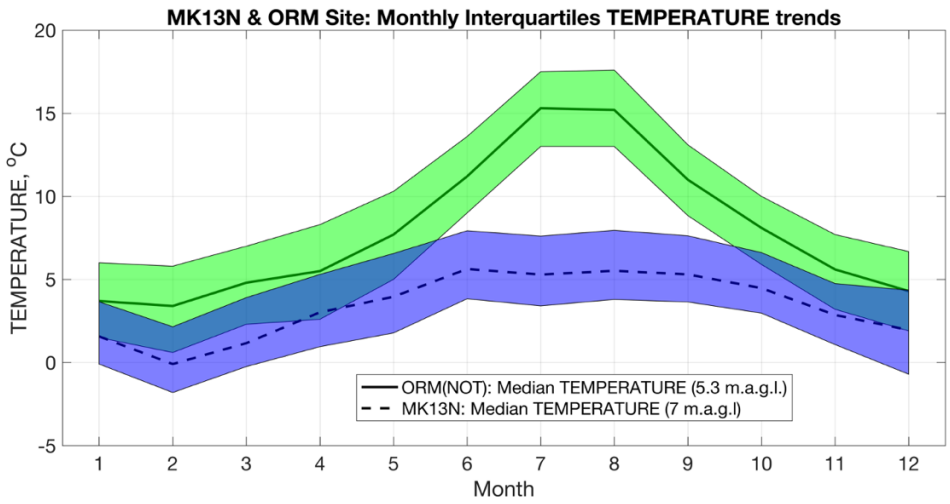

Figure 2: Seasonal variation of the median temperature at ORM and MK13N *(magl=meters above ground-level)*

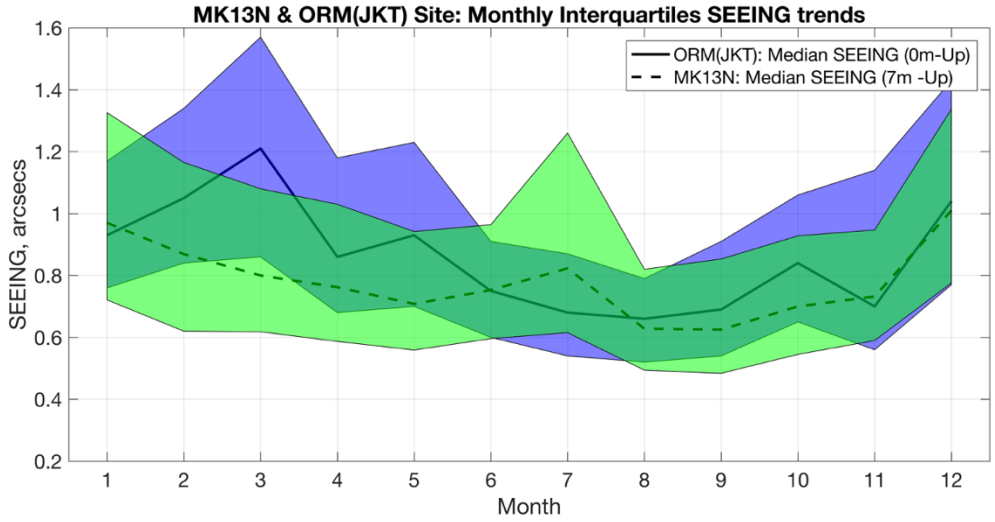

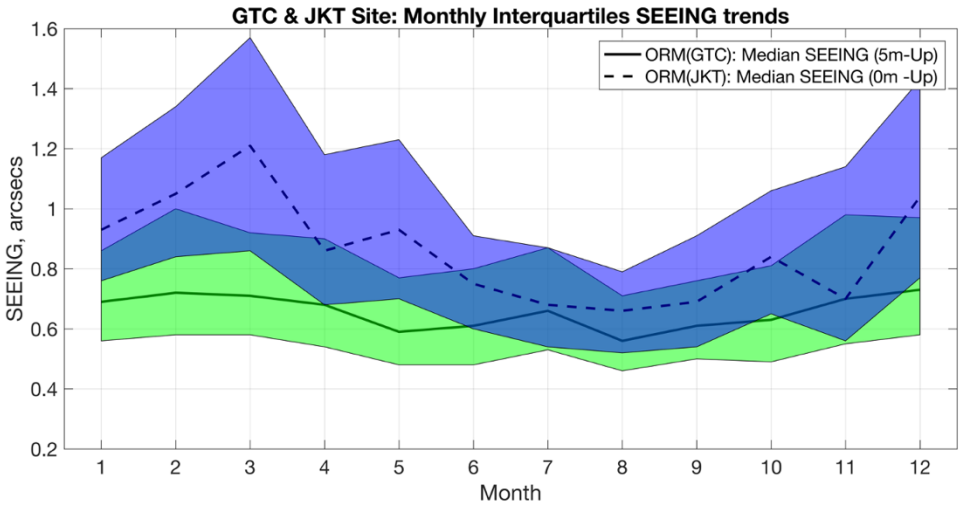

Figure 3: Top: Seasonal variation of total seeing at ORM (median value, from JKT/g-Scidar measurements) and MK13N. Bottom: Yearly seeing variation measured at the JKT (g-Scidar data analyzed in this report) and GTC (DIMM data, prior to construction) sites.

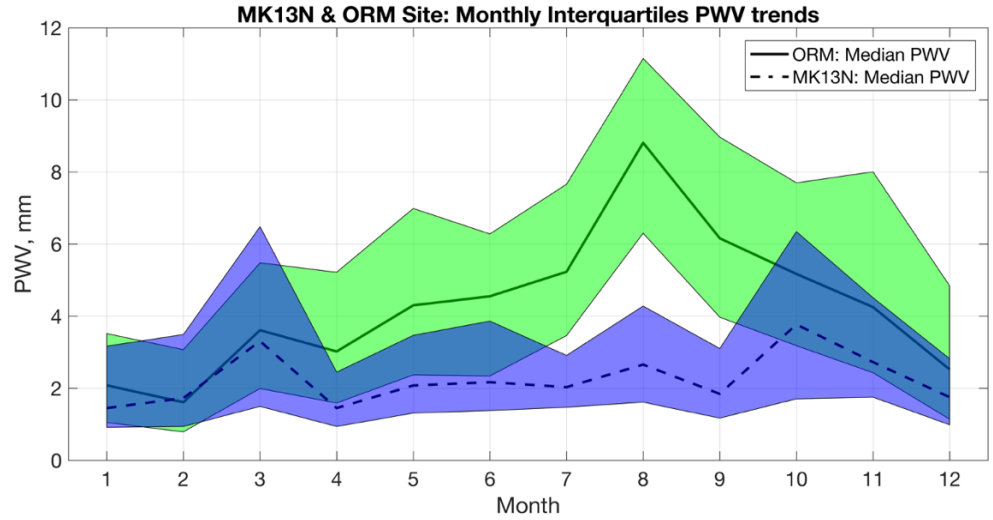

Figure 4: Seasonal variation of PWV at ORM (see section 1.2.2) and MK13N.

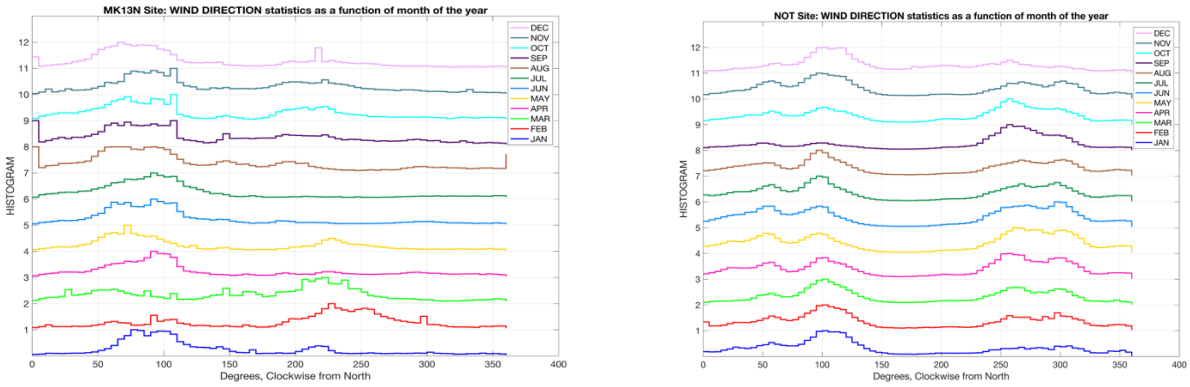

Figure 5: Seasonal variation of wind direction at MK13N (left) and at ORM (right figure, at the site of the Northern Optical Telescope site).

In **Figure 6** we plot the monthly trends of the median statistics for PWV, seeing, temperature and available nights for observations at the ORM site. To make the plot easier to read, the range of each variable has been adjusted to fit within a unique vertical range (see figure insert). The figure shows that the first part of the summer is drier than the second half. Also, seeing is better in summer while the driest conditions happen in wintertime.

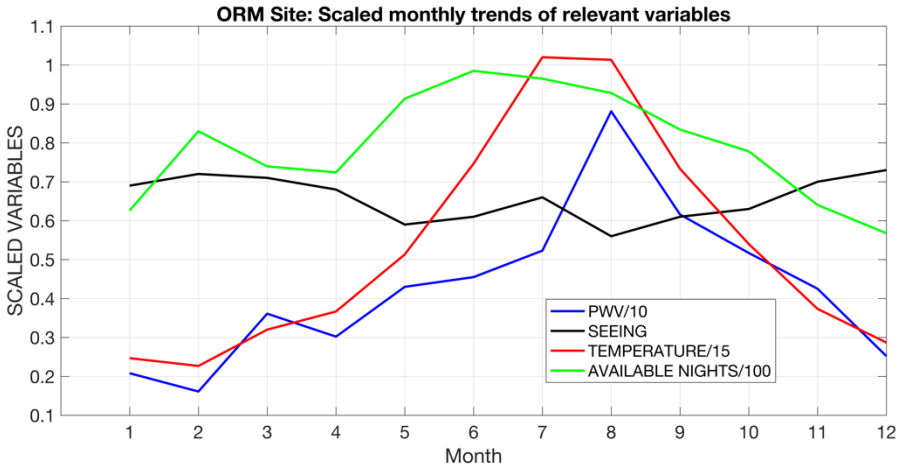

Figure 6: Seasonal variation of the median values of key parameters: PWV (see section 1.2.2), seeing (from GTC), temperature and available nights at the ORM site.

1.1.3. Information about Seeing and Turbulence Profiles

The measure of the seeing informs us on the state of the turbulence of the atmosphere above the Observatory. Factors characterizing the turbulent state of the atmosphere deal with the size of the coherent atmospheric cells (atmospheric coherence length and isoplanatic angle) and the duration over which atmospheric cells will modify the wavefront of the light (atmospheric

coherence time). The smaller the seeing, the better the quality of the site for carrying out astronomical observations, while a more stable atmosphere (long coherence time, large isoplanatic angle) will facilitate the adaptive optics correction of the wavefront of the light, improving considerably the quality of the AO images delivered to the science instruments.

The Narrow Field Adaptive Optics System (NFIRAOS) is the TMT adaptive optics (AO) facility instrument. Its design is based on the principles of Multi-Conjugate Adaptive Optics (MCAO), which provides AO correction over a ~2 arcmin field using a set of natural and laser guide stars surrounding the scientific target. NFIRAOS correction is based on the turbulence measurements obtained by wavefront sensors and the operation of two deformable mirrors optically conjugated to the turbulence at the ground and upper troposphere layers, the two atmospheric layers that contribute most to the aberrations of the wavefront of the light (Herriot et al., 2010).

Measuring the strength of the turbulence profile as a function of altitude is thus extremely important to understand the characteristics of any site and how good that site is for using adaptive optics. In this context, during the original 2004-2008 site survey, the TMT project measured the boundary layer atmospheric turbulence and wind profiles for all potential sites using SOnic Detection And Ranging (SODAR) acoustic sounders (Travouillon et al., 2006). Considering that the TMT dome reaches ~60 m above the surface, the turbulence profile close to the ground was probed using two types of SODAR, one returning measurements in the range from 40 m to 800 m above the ground, with 20 m vertical resolution, and another instrument returning a finer vertical resolution of 5 m and probing the turbulence in the range from 5 m up to 200 m above the ground. Information about the higher turbulent layers was accessed by combining DIMM data (integrated seeing) and MASS data (vertical profile of turbulence) measured contemporaneously with the SODAR measurements.

Figure 7 below shows the median seeing measured by the TMT team as a function of height above the ground at four different sites (Maunakea - USA, Armazones and Tolonchar - Chile, San Pedro Martir – Mexico) during the pre-2008 site-testing period. This figure is extracted from Schoeck et al., 2009 (figure 3 of the referenced paper). It clearly shows the increase of integrated seeing in the boundary layer as one gets closer to the surface. Previous Computational Fluid Dynamic (CFD) simulations showed that the turbulence below the top of the enclosure (i.e. below 60m) is itself dominated by the design of the enclosure (Vogiatzis et al. 2018). As a result, we removed from our profiles the turbulence corresponding to an altitude below 60 m to model the expected image quality delivered by NFIRAOS (an extra term for dome and mirror seeing can later be added to the simulation results). For that purpose, we estimated the fraction of the [DIMM – MASS] turbulence strength that is above 60 m altitude using the median SODAR profiles we had measured. We then reduced the ground layer (GL) turbulence of each individual MASS/DIMM profile by this fraction[1]. These new GL-strength-reduced profiles were then averaged to produce median (or percentile) representative profiles. A close look at **Figure 7** shows an interesting feature of the turbulence in the boundary layer: the sites located on mountain peaks (such as Armazones and Tolonchar) display a different, shallower, surface layer than the sites located on slopes (such as MK13N and San Pedro Martir). In addition, the shape of the individual profiles (when normalized to the same MASS and DIMM seeing) are very similar within each of these two categories (slope and peak).

[1] While it would have been preferable to reduce the GL of a profile using simultaneous SODAR measurements, this is not possible for the entire data set because the SODAR data at all sites span a much shorter amount of time than the MASS/DIMM profiles. However, as GL and free atmosphere turbulence are only weakly correlated, using the median SODAR profiles instead produces accurate long-term statistics.

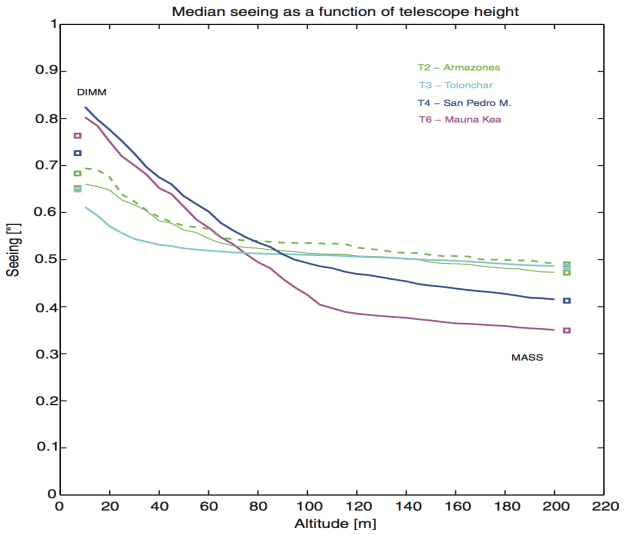

Figure 7: Median seeing an observer would experience at a given altitude above the ground as calculated from the MASS, SODAR and DIMM turbulence measurements (simultaneous data only), from 7 to 200 m above the ground. There are two curves plotted for Armazones as two SODAR instruments were used simultaneously.

SODAR measurements of the boundary layer have not been gathered at the ORM site. Still, based on the analysis of **Figure 7** above and the fact that ORM is located on the western slope of the Roque de Los Muchachos, it is expected that the average boundary layer turbulence profile at ORM should be similar to that of MK13N. As a result, and in the analysis that follows, we have reduced the GL strength of the ORM turbulence profiles by the same factor we have used for MK13N.

Table 4: Statistical distribution of seeing at ORM (total seeing, ground-layer, free-atmosphere, seeing at 60m and ground-layer at 60m).

Percentile	Total Seeing	Total Ground-Layer	**Seeing 60m & up**	Ground-Layer 60m & up	Free Atmosphere
25%	0.64	0.44	**0.45**	0.22	0.32
50%	**0.82**	**0.64**	**0.58**	**0.33**	**0.4**
75%	1.13	0.94	**0.75**	0.48	0.52
95%	1.62	1.39	**1.09**	0.71	0.82

Table 4 above shows the latest analysis results from the g-SCIDAR data, reporting the percentile seeing distribution (total seeing, ground layer, and free atmosphere). Values for the 60m-up seeing are also calculated. The total integrated seeing has a median value of 0.82", which is reduced to 0.58" at the 60m height of the enclosure. For comparison, we also include in **Table 5** below the values for the 60m seeing and ground-layer, and free atmosphere at MK13N, ORM and Armazones. ORM has a stronger ground-layer than MK13N and Armazones, but smaller free-atmosphere seeing than Armazones.

Table 5: Comparison of statistical seeing distribution at MK13N, ORM and Armazones.

Percentile	Maunakea 13N			ORM			Armazones		
	Seeing (60m and up)	Ground layer (60m)	Free atmosphere	Seeing (60m and up)	Ground layer (60m)	Free atmosphere	Seeing (60m and up)	Ground layer (60m)	Free atmosphere
25%	0.37	0.19	0.22	0.45	0.22	0.32	0.38	0.11	0.31
50%	**0.50**	**0.27**	**0.34**	**0.58**	**0.33**	**0.40**	**0.50**	**0.16**	**0.44**
75%	0.70	0.38	0.52	0.75	0.48	0.52	0.69	0.23	0.63
95%	1.33	0.66	1.18	1.09	0.71	0.82	1.14	0.40	1.09

The next figure (**Figure 8**) shows a comparison of the median turbulence profiles (Cn^2xdh) between ORM (from the analysis of the g-SCIDAR/JKT data) and Armazones and MK13N (from Schoeck et al. 2009). The stronger ground-layer of ORM and MK13N in comparison to Armazones is clearly visible.

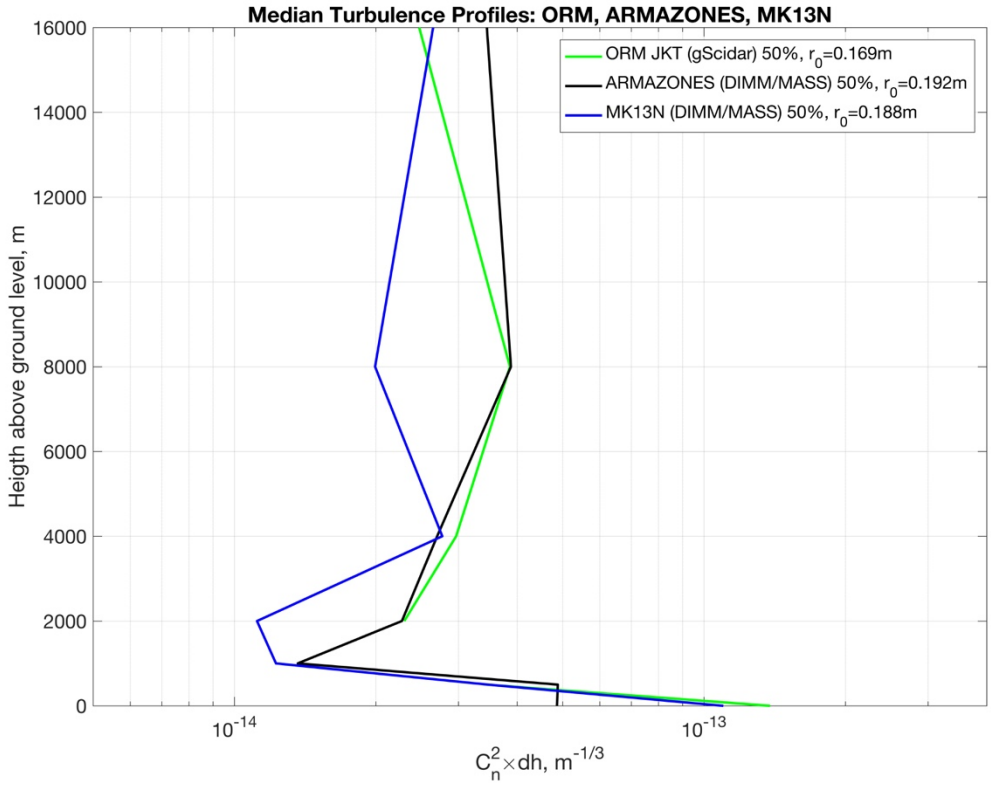

Figure 8: Comparison of the median turbulence profile of ORM, MK13N and Armazones

1.1.4. Atmospheric Coherence Time and 200 mbar Wind Speed

The turbulence coherence time, τ_0, describes how fast the wavefront error at the telescope pupil changes. This parameter has an important effect on the performance of adaptive optics systems, in particular for high-contrast science programs. Although τ_0 results from the integrated turbulence of all atmospheric layers, the layer contributing most to τ_0 is located high in the troposphere, at approximately 12 km above sea level, at a corresponding atmospheric pressure of ~200 mbar (altitude of the jet stream).

The 200 mbar wind speed at many observatory sites has been studied extensively (see, for example, García-Lorenzo et al., 2005, or Bounhir, 2009, and references therein). García-Lorenzo et al. (2005) shows that ORM and Maunakea have the lowest 200 mbar wind speeds among major observatory sites. From **Table 6** (which is extracted from García-Lorenzo et al., 2005), it is shown that the mean, median and standard deviation values of the 200mbar wind speed above Maunakea and ORM are very similar, with values for ORM being 5-10% lower than for Maunakea. In comparison, Armazones displays higher 200mbar wind speed values, due to a stronger jet stream presence above Northern Chile. ORM and Maunakea's monthly statistics are also very similar, with the only significant difference in winter and early spring, when Maunakea wind speeds are somewhat larger than ORM's (see figure 2 from García-Lorenzo et al., 2005).

The JKT g-SCIDAR turbulences data studied in this report do not include measurements of τ_0 but, given the similarity of the turbulence profiles between MK13N and ORM, we can expect τ_0 for ORM to be similar to that of MK13N, and the 6ms value for τ_0 listed in **Table 2** is a conservative estimate of the coherence time at ORM. The long coherence times of MK13N and ORM make them excellent sites for Extreme-AO observations.

Table 6: 200 mbar wind speed statistics for the two Northern TMT sites MK13N and ORM. The data for the E-ELT site are also included for comparison. Values are from García-Lorenzo, 2005. Paranal values are used for Armazones, as the free-atmosphere wind is a large-scale phenomenon.

Site Characteristics (median values, unless stated)	MK13N (USA)	ORM (Spain)	Armazones (Chile)
Median 200 mbar wind speed (m/s)	22.8	20.8	28.6
Mean 200 mbar wind speed (m/s)	24.3	22.1	30.1
Monthly standard deviation (m/s)	12.3	11.7	13.0

1.1.5. The Site Merit Function

A Site Merit Function, SMF, (Schoeck et al. 2011) was developed during the 2004-2008 TMT site study. The same function for the visible and near-infrared (see **Table 7**) was used in this recent study to quantitatively compare the relative merit of each alternate site for the main TMT observing regimes: seeing-limited observations in the visible range, near-IR observations with/without the support of adaptive optics, and mid-IR observations. Note that for the mid-IR regime, we adopted a revised and more comprehensive form of site merit function than for our earlier study. This new approach has the effect of amplifying the difference between each site to support mid-IR observing modes (based on their PWV, pressure and temperature).

We used the following realistic weighting between observing regimes for calculating the total SMF for each site: 40% visible, 50% near-IR and 10% mid-IR. To emphasize the comparative aspect of this study, the SMF values were normalized to 1 for MK13N. The SMF uncertainty is of the order of 10%.

This merit function shows that ORM will perform well in the visible and near-IR ranges, which are the wavelength regimes where the core TMT science is expected to be done. At mid-IR wavelengths, the site merit function confirms that TMT at MK13N will outperform TMT at ORM, emphasizing the importance to carry out such programs when atmospheric conditions are most adequate. TMT science programs will be implemented and executed at the Observatory using a conditions-based adaptive scheduling engine, which will ensure that the most demanding programs are executed when the required weather conditions are met. This will result in a much higher mid-IR performance of ORM than shown in **Table 3.** Note that the SMF takes into account the main site parameters previously defined in **Table 2.**

Table 7: Site merit function metrics for typical observing conditions (i.e. "classically scheduled", prior to any scheduling optimization with adaptive queue). The values are all normalized and compared to MK13N (the higher the number, the better is the site for a specific observing regime). ORM data *(in italic)* * refer to the analysis of the ESO E-ELT's site MASS-DIMM measurements, which were obtained closer to the TMT location than the g-SCIDAR measurements used in our own analysis, but cover a shorter time period.

Site Merit Function (normalized to KN13N)	**MK13N**	**ORM**	**ARM**
Visible (seeing-limited) metric	1.00	0.81 *(1.00)**	1.19
Near-IR metric	1.00	0.74 *(0.76)* *	0.95
Mid-IR metric	1.00	0.18 *(0.18)* *	0.80
Total Metric	**1.00**	**0.71 *(0.80)*** *	**1.03**

1.2. ASTRONOMICAL OBSERVATIONS WITH THE TMT AT ORM

The Observatorios de Canarias, consist of both the Observatorio del Roque de Los Muchachos (ORM), situated on the island of La Palma, and the Observatorio del Teide, located on the island of Tenerife. Jointly, these observatory sites include the telescopes and astronomical instrumentation of about 60 research institutes from more than 20 countries. Both sites are protected from light-pollution and a continuous effort is carried out to preserve the photometric quality of the night sky. Also, very importantly, the areas above and around the two sites have

been declared a no-fly zone by any commercial aircraft (Talbot et al. 2006). Such regulations tremendously facilitate the operations of laser guide stars, entirely preventing the interruption of AO/LGS assisted observations due to aircraft flybys.

All spectral bands that can be observed with ground-based instrumentation (high-energy astrophysics, visible, near-infrared and mid-infrared, as well as cosmic background in radio wavelengths) are used throughout the Teide and ORM observatories. ORM itself is already the site for 12 telescopes with a large range of apertures, including the 10.4m Gran Telescopio Canarias (GranTeCan). ORM is also the site for the Cherenkov Telescope Array (CTA; Hermann et al., 2007; Castro-Almazan et al., 2018). **Table 2** above compared a number of properties for ORM and Mauna Kea. The ORM site can support all TMT core-science goals, though with lower sensitivity than Maunakea at some wavelengths in the UV and mid-IR. The number of expected usable nights is equal for both sites.

The sections below describe in details the impact on adaptive optics (NFIRAOS) assisted observations at ORM in comparison to MK13N in the near-infrared and mid-infrared regimes.

1.2.1. Near-Infrared AO Observations: TMT performance at ORM

1.2.1.1. History of AO programs at ORM

ORM has had a significant and pioneering role in the historical development of the adaptive optics technique. Solar AO has been routinely performing AO-serviced science observations since 1999 at the Swedish Solar Telescope (SST) with great success, producing the best obtained images of solar granulation from the ground (until the advent of DKIST). SST's 3rd generation AO system was revamped in 2013 and features a wavefront sensor (WFS) with 9.4 cm hexagonal sub-apertures closing the loop at 2 kHz, which allows diffraction limited solar images to be obtained in variable seeing conditions (Schärmer et al. 2019). Bearing in mind that solar telescopes have to observe at very low elevations, early in the morning, when conditions mirror those of nighttime, and at mid-day when the seeing varies most rapidly and is much worse than at nighttime, the amazing solar science results obtained with the AO system of the SST is strong proof that the ORM site is very well suited for AO-fed instruments.

Regarding nighttime AO, the first tomographic all-sky AO reconstruction, and the first on-sky test of a pyramid WFS, were achieved at the ORM in 1999 and 2000 (Ragazzoni et al, 2000a; Ragazzoni et al, 2000b). These results were obtained with the AO facility at the 3.6m Telescopio Nazionale Galileo (TNG).

Other AO experiments at the ORM include NAOMI and Canary: NAOMI (Myers et al, 2003) is a Ground Layer AO system for the 4.2m William Herschel Telescope (WHT) that was upgraded with a 20W Rayleigh laser guide star (LGS) in 2008 (Benn et al, 2008). Canary is the AO demonstrator for the European Extremely Large Telescope (E-ELT). This system was set up at the WHT after several campaigns confirming the excellent conditions for AO at the ORM (Martin et al, 2014). Canary, which is based on a 20W Na WLGSU (Wendelstein Laser Guide Star Unit) located 39m

away from the center of the pupil of the WHT, is crucial for the validation of LGS wavefront reconstruction for the ESO E-ELT (Bardou et al, 2018).

Still, despite the excellent quality of the site to conduct AO observations, some lack of instrument funding prevented the development of AO systems dedicated to nighttime scientific observations. This paradigm is about to change with the upcoming (2020-2021) installation of the first AO system at the GTC (GTCAO), which will feed the FRIDA instrument (a near-IR imaging integral field spectrograph), thus enabling science cases requiring the full diffraction-limit power of a 10m class optical-infrared telescope.

1.2.1.2. SIMULATION OF AO PERFORMANCE WITH TMT/NFIRAOS

TMT has been conceptually conceived and designed to be highly optimized in the near-infrared spectral bands, achieving high Strehls and low background noise to provide the capabilities required to conduct those TMT science cases that utilize near-IR AO observations. The TMT design of the AO facility instrument NFIRAOS is based on Multi-Conjugate Adaptive Optics (MCAO), which includes two deformable mirrors (conjugated at ground-level and at an altitude of 11.6km) to compensate for the adverse effects of high altitude and ground layer turbulences, while reducing the number of optical surfaces, all in an actively cooled environment to minimize thermal background. Only TMT's primary, secondary and tertiary mirrors are left at environmental temperature conditions and their coating has been selected to maximize reflectivity in the near- and mid- infrared spectral bands.

As discussed earlier, the values of the isoplanatic angle and coherence time for ORM and Maunakea confirm that near-IR adaptive optics observations are expected to be particularly effective at both the MK13N and ORM sites (see adaptive optics Strehl merit value in **Table 2**). In this respect, we used performance modeling with the Multi-Threaded Adaptive Optics Simulator (MAOS) software (Wang & Ellerbroeck, 2012) to estimate and compare the relative sensitivity of TMT/NFIRAOS at both sites. It is important to note that this relative sensitivity corresponds to the inverse of the integration time needed to reach the same signal to noise ratio at both sites.

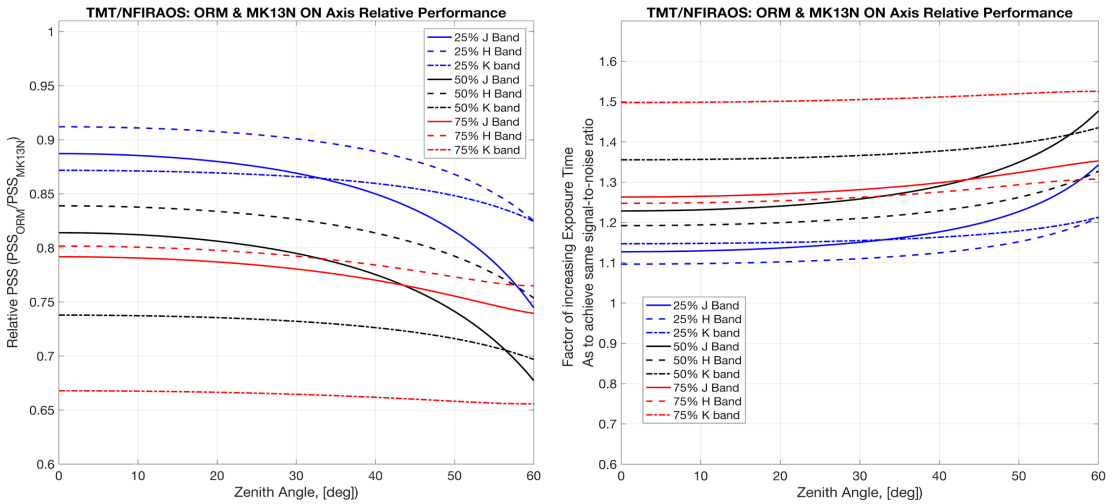

Figure 9: (Left) Relative Point Source Sensitivity of TMT/NFIRAOS in the J (1.1-1.4μm), H (1.5-1.8μm), and K (2.0-2.4μm) spectral bands between the ORM and MK13N sites. (Right) Factor of increasing observing time for ORM in order to achieve similar S/N ratio as at the MK13N site.

Figure 9 shows the ratio of sensitivity between MK13N and ORM as a function of the observing wavelength and zenith angle (on-axis case), together with the exposure time increase required at ORM to reach the same sensitivity as at MK13N. This calculation takes into account the characteristics of the site such as a lower transparency and higher thermal background for ORM in comparison to MK13N. For on-axis observations under the best AO conditions, with a zenith angle varying from 0 to 45 degrees, the integration times for ORM observations only need to be increased by 15% at most to achieve the same S/N than for MK13N (in all spectral bands). For the less optimal cases of 50% and 75% turbulence conditions, and for J and H spectral bands (worst turbulent conditions), the additional increase in observing time is less than 30%. For K-band, which is the most sensitive to thermal atmospheric background in the near-infrared range, targets as low as 50 deg. zenith angle can be observed from best to median atmospheric conditions with the same S/N as MK13N by increasing the exposure times by less than 40%.

Assuming that the most exceptional science will be obtained during the best conditions, and considering that adaptive queue scheduling will provide the best conditions to the most challenging programs, the above figures shows that ORM can support such high-impact science observations with a very modest ~ 15% increase of exposure time.

Figure 10 below shows the residual wavefront errors, accounting only from the differences in the strength and vertical distribution of atmospheric turbulences between the two sites. All other factors affecting the NFIRAOS performance are taken to be site-independent, and consequently ratio out. The residual WFE is reported for various zenith angles, up to 65 deg, and several turbulence regimes (best 25%, median conditions, and 75%).

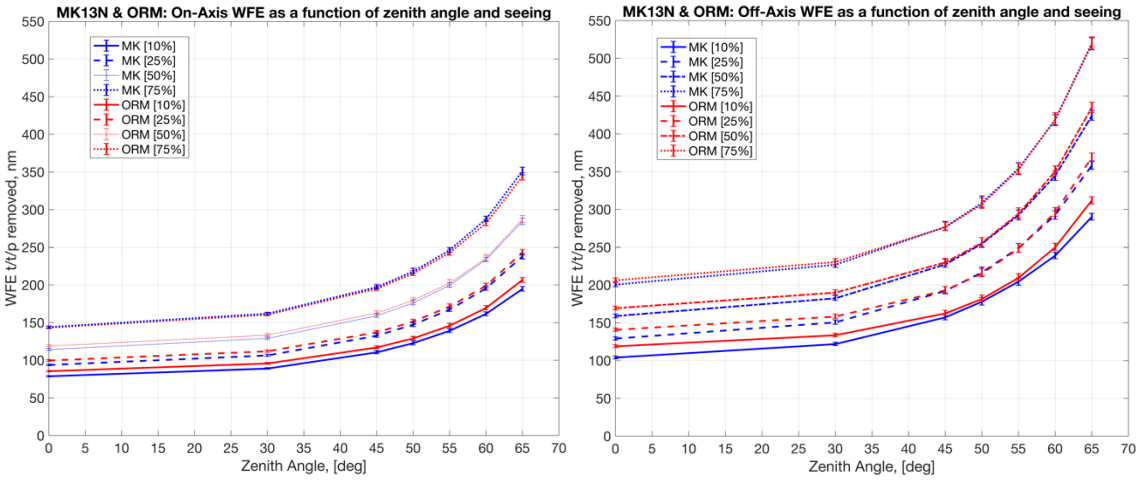

Figure 10: MAOS estimates of the on-axis (left) and off-axis (right) NFIRAOS wavefront error (WFE) due to atmospheric turbulence at ORM and MK13N. The off-axis WFE is averaged over regions on the edge of a 34x34 arcsecs field centered around the optical axis. Implementation

errors (additional 152 nm)[2] due to the AO system (from NFIRAOS wavefront error budget) are not included in these figures as these are site independent.

In terms of achievable Strehl ratios,

It is also interesting to note that, at high zenith angles, TMT at ORM shows superior performance to that expected from TMT at Armazones. This is most likely due to a stronger effect of upper-troposphere turbulences at Armazones (due to the jet stream wind pattern). To pursue this comparison, TMT/NFIRAOS at ORM is also fully competitive with respect to the other ELTs: E-ELT and GMT. These two other projects announce expected on-axis WFE at zenith of 350nm (GMT, Sitarski et al., 2019) and 265nm (E-ELT construction proposal), implying Strehls in K-band of the order 37% and 56% respectively (to be compared with 74% for TMT at ORM from our simulations).

Figure 11 plots the expected absolute Strehls that TMT/NFIRAOS can reach at ORM as a function of wavelengths and target zenith angle (for median conditions). The results for ORM were obtained using the median turbulence profile from the JKT data reported in this document. MK13N and Armazones (the site of the ESO E-ELT) are also shown for comparison (the turbulence profiles of MK13N and Armazones were obtained by the TMT site testing team, Schöck et al., 2009). These simulations show that the relative efficiency of TMT/NFIRAOS/LGS at ORM is fully comparable with that expected for the MK13N and Armazones sites, with similar performances over the full range of zenith angles.

It is also interesting to note that, at high zenith angles, TMT at ORM shows superior performance to that expected from TMT at Armazones. This is most likely due to a stronger effect of upper-troposphere turbulences at Armazones (due to the jet stream wind pattern). To pursue this comparison, TMT/NFIRAOS at ORM is also fully competitive with respect to the other ELTs: E-ELT and GMT. These two other projects announce expected on-axis WFE at zenith of 350nm (GMT, Sitarski et al., 2019) and 265nm (E-ELT construction proposal), implying Strehls in K-band of the order 37% and 56% respectively (to be compared with 74% for TMT at ORM from our simulations).

[2] In order to get the total WFE, the residual WFE shown in the plots (for any zenith distance of interest, as well as atmospheric turbulence condition) needs to be added in quadrature to the implementation error of 152 nm. WFE_total = sqrt(152^2 + WFE^2), where WFE is extracted from Figure 4.

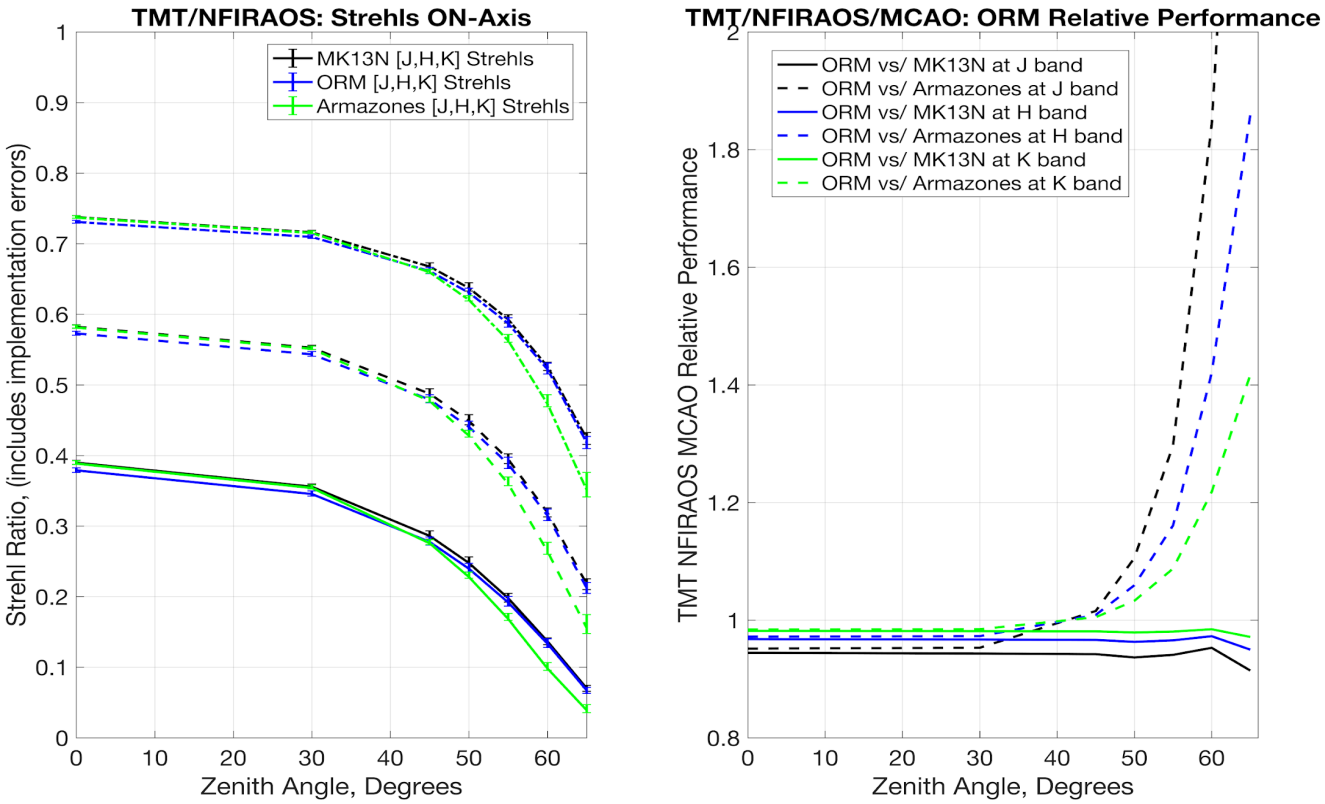

Figure 11: (Left): TMT/NFIRAOS absolute Strehls in J, H, and K spectral bands, based on the median turbulence profiles and isoplanatic angle θ_0 (above 60m) known for the MK13N, ORM and Armazones sites. (Right): Relative performance (ratio of Strehls at the J, H and K spectral bands) of TMT/NFIRAOS in MCAO mode at ORM compared to MK13N and Armazones.

1.2.2. Thermal and Mid-Infrared Observations

In comparison to MK13N, TMT at ORM will provide lower sensitivity at thermal and mid-IR wavelengths. This is due to the lower altitude of the ORM site, which results in increased molecular line broadening produced by higher atmospheric pressure and temperature, and a larger percentage of precipitable water vapor in the atmosphere. High altitude, cold, and dry sites like MK13N provide a larger fraction of nights when the conditions are favorable for mid-IR astronomical observations. The high altitude (lower atmospheric pressure) helps with decreasing the pressure broadening of atmospheric absorption lines, the colder temperatures help minimizing the thermal background noise, while a dry atmosphere (low absolute humidity) minimizes the absorption of astronomical radiation by water vapor molecules along the telescope's line of sight.

Still, mid-IR observations at ORM can be successfully carried out, but should be obtained when the weather conditions are among the driest for this site (lowest percentage of precipitable water vapor). To a large degree, this can be addressed by TMT's operations model which will include flexible scheduling, allowing to rapidly switch to mid-IR TMT instrumentation whenever the

ambient conditions are favorable, hence taking advantage of the windows when mid-IR sensitivity is at its highest level. In the thermal-IR and mid-IR ranges (wavebands where atmospheric water vapor, as well as atmospheric temperatures, start to play an important role) 3-25 μm instruments have also been successfully deployed at astronomical observatories with elevations similar to ORM's: Gemini-South (NIRI, GNIRS, Phoenix), ESO-VLT (ISAAC, CRIRES, VISIR), MMT (MIRAC) and Gran Telescopio Canarias (GTC; CanariCam).

As of today, and thanks to accurate atmospheric forecasts, the operations and scheduling of astronomical observations already enable very demanding astronomical observations (e.g. thermal and mid-IR science programs that need cold and dry atmospheric conditions) to be conducted. In addition to on-site measurements, TMT will utilize forecasting of atmospheric conditions (wind, temperature, seeing, precipitable water vapor) to support flexible queue-scheduling of astronomical observations, including at wavelengths longer than 3 μm. Such forecasting of meteorological conditions is already partly in place at ORM.

Table 8 lists the PWV and atmospheric temperature statistics for ORM and MK13N. For ORM the statistics come from the analysis of 2 years (2012 and 2013) of radiosonde data integrated from the altitude of the ORM site and above. The MK PWV statistics come from the analysis of 4 years of PWV derived from 225 GHz optical depths at the location of the Caltech Submillimeter Observatory (CSO). **Figure 12** is a graphic representation of the data from **Table *8***.

Table 8: Statistics of the Precipitable Water Vapor and Nighttime Temperature for ORM and Maunakea.

Percentile	MK13N (4050m)		ORM (2250m)	
	PWV (mm)	Night Temp. (˚C)	PWV (mm)	Night Temp. (˚C)
5%	0.6	-2.3	1.0	-1.9
10%	0.8	-1.3	1.4	-0.8
25%	1.1	+0.4	2.2	+2.8
50%	1.9	+2.3	4.2	+8.1
75%	3.5	+3.9	7.0	+11.9

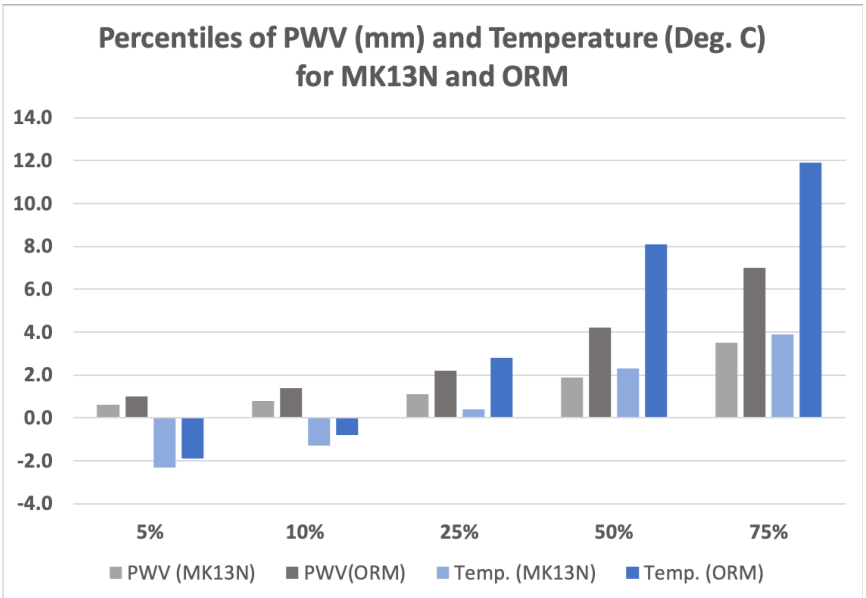

Figure 12: Representation of the statistical distribution for Precipitable Water Vapor and Nighttime Temperature for ORM and Maunakea – from **Table 8**.

As done for the near-IR regime, our modeling allows us to estimate the increase in observing time for ORM that TMT thermal/mid-IR observations will require to achieve the same S/N ratio as at MK13N. The mid-IR radiative transfer simulations were done for a variety of different conditions and are described in detail in a companion technical report to this document (TMT Mid-IR Sensitivity Analysis – TMT-MIRSA 2021). The results shown in **Figure 13** are one example taken from that report, using the 25-percentile of PWV and temperature conditions, assuming observations are made at 30° zenith angle and a local thermal background for the telescope and instrument equivalent to 11% optics emissivity.

Weather forecasts of PWV and temperature are comparatively easy to obtain over time scales of a few hours. Considering that only 10% of TMT observing time is expected to be spent on MIR observations, such programs can be scheduled within the 25-percentile of best atmospheric conditions. The differences in MIR performance between the MK13N and ORM sites decrease further from those in the figure when observations are made at better than 25-percentile conditions, as shown in TMT-MIRSA (2021). In addition, the 11% emissivity used in our model corresponds to completely clean and freshly coated mirrors. As mirror coatings age and accumulate dust, their emissivity increases, resulting in a larger local thermal background which further decreases the mid-IR sensitivity differences between the two sites. Thus, the results in **Figure 13** are an upper limit to the expected differences between the two sites.

The results shown in **Figure 13** further illustrate that sensitive mid/thermal-IR observations are possible at the ORM site. Many MIR observations concentrate on the transparent regions of the spectra between atmospheric lines. For these regions, the lower envelope of the curves is the relevant metric for comparing site performance. For broadband imaging, an integral of the curves over the wavelength range of the filter provides the corresponding sensitivity. Note that the spectra shown in **Figure 13** do not have a high enough resolution at long wavelengths to accurately report on mid-IR site comparison for narrow atmospheric lines. Similar simulations can

be run using the appropriate resolution to carry out this analysis. More information is given in TMT-MIRSA (2021).

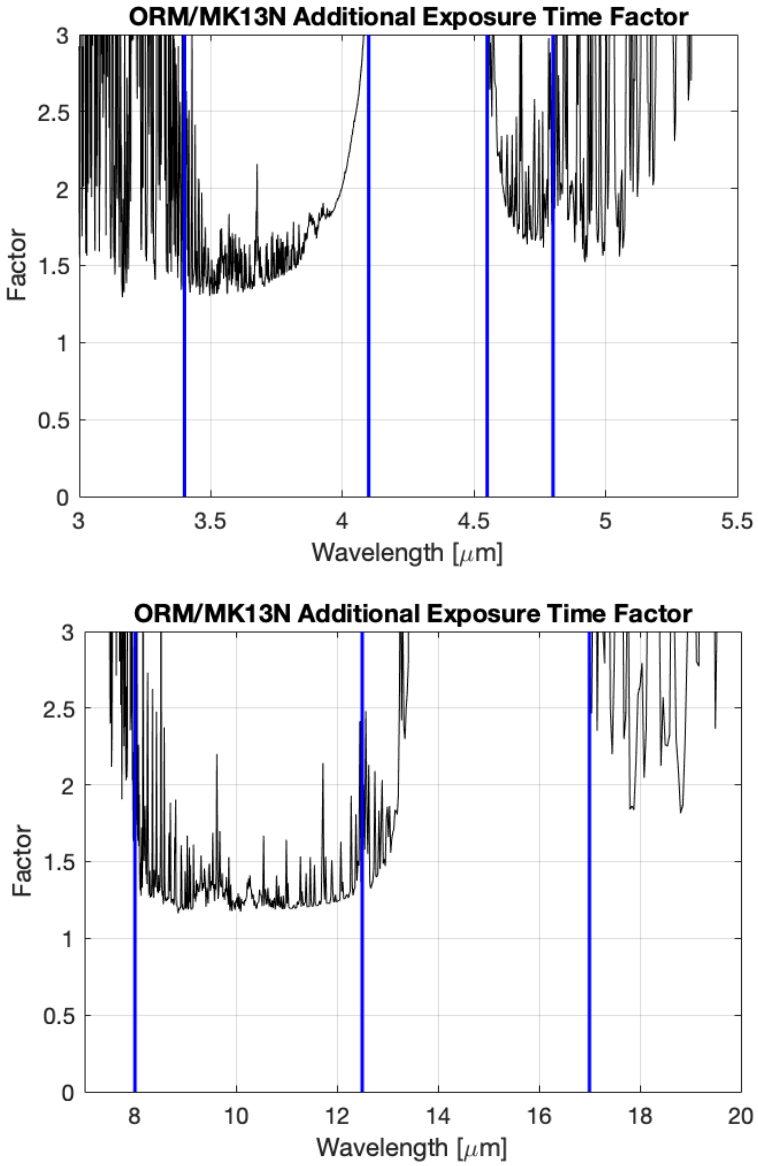

Figure 13: MIR sensitivity for L and M band (top), and N and parts of Q band (bottom) using 25-percentile conditions of PWV and nighttime temperature, 30° zenith angle and optics emissivity of 11%. The plots show the additional exposure time factor needed to reach the same S/N ratio at ORM as at MK13N. The vertical lines in the plots indicate the limits of the L' (3.4–4.1 µm), M' (4.55–4.8 µm), N (8–12.5 µm) and Q (17–25 µm) bands.

1.2.3. UV Region of the Optical spectrum

For science programs that utilize observations at the shortest wavelengths (0.31µm to 0.34µm), we can consider that the impact of the lower altitude of ORM is relatively small. Indeed, comparison of the extinction curves for both sites (**Figure 14** below) shows that the same level of extinction between ORM and MK13N only occurs at wavelengths about 5nm shorter for ORM (the transmission at ORM is about 2/3 that of MK13N at 340nm). This 5nm difference would affect programs observing redshifted Lyα, as a redshift difference of 0.04 corresponds to about 100 Myr. There are also line features in the spectra of galactic ultra-metal poor stars in the 0.310µm to 0.325µm region that would be affected.

Currently, the main limitation at this wavelength regime is rather of a technical nature, and it affects similarly MK13N and ORM. It is due to challenges in producing highly reflective mirror coatings and optics in the UV. When coating technology is improved, allowing better reflectivity in this region of the spectrum, then we estimate that observations in the 0.31µm to 0.34µm will require up to 50% longer exposure times at ORM in comparison to MK13N.

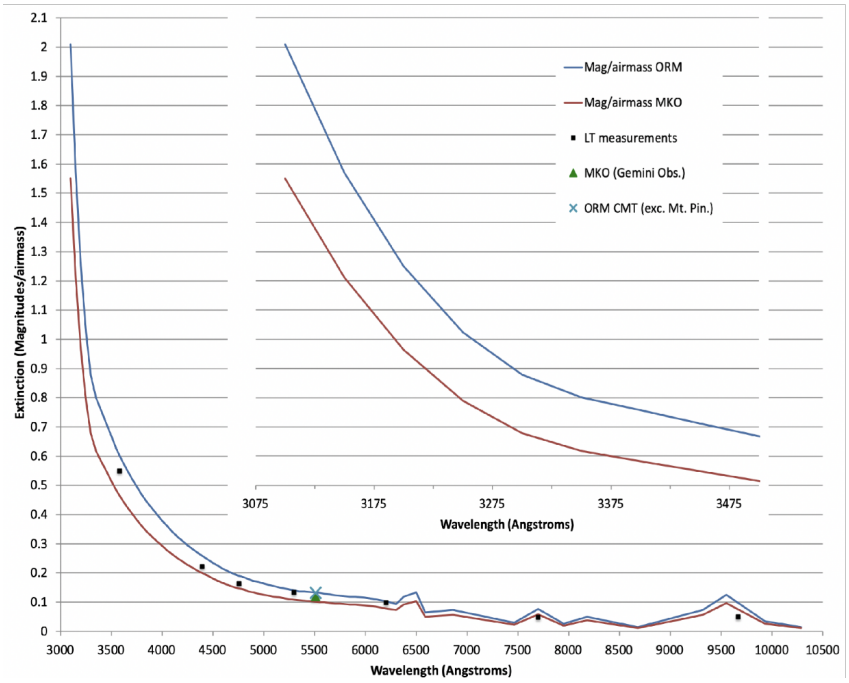

Figure 14: UV extinction curves modeled by Chuck Steidel (consistent with his calibration measurements at ORM and Maunakea) and shown against measured extinction values from ORM (Liverpool Telescope and Carlsberg Meridian Telescope) and Maunakea. Differences between extinction at ORM and Maunakea at wavelengths longer than 5000 Ang. are at the 2% level or less. The inset shows the short wavelength range, where the equivalent transmission at ORM occurs at a wavelength about 5nm shorter than at Maunakea. At 340nm, the transmission at ORM is 2/3 that at Maunakea.

1.2.4. Effect of Dust

There is a perception in the astronomical community that ORM is heavily compromised by the presence of dust. Our analysis of (i) over 14 years of dust measurements at ORM, and (ii) the impact of dust on observatory operations (weather loss, mirror reflectivity degradation, impact on other observatory systems) shows that dust does not have a significant effect that would be a discriminating factor for ORM. To better comprehend the impact of dust, let's consider the two potential consequences of dust at a site:

- One is due to dust at "ground level", which can potentially affect instrumentation, primary mirror sensors and actuators, and the cleanliness of optics. There is no evidence from our analysis of long-term dust measurements and observing logs of telescopes in operation (several years of photometric zero points at the Liverpool Robotic Telescope) that observatory-level dust causes reduced efficiency, or any loss of observing time other than that accounted for in the usable time statistics. In spite of the known sporadic episodes of Sahara dust reaching the Canary islands at sea-level, **Table 9** shows that the dust levels statistics at the altitude of ORM are comparable to MK13N and the effect of dust on telescope optics is found to be comparable between sites (see Annex II subsection 5.1).
- The second is due to dust at higher altitude in the atmosphere, which can increase extinction, particularly at shorter wavelengths and during the summer. **Table 2** shows that the average extinction statistics for usable nights, regardless of cause, are equivalent to those of MK13N. Note that the usable time estimates in the table already include both the case when extinction due to high-level dust is so large that observations become inefficient, and also when ground level dust concentrations are too high to keep telescope operations running (no additional contribution from dust needs to be added).

The implications of dust at ORM, including near surface dust particle concentration, as well as atmospheric extinction (higher altitude) was addressed in detail in our original alternate site study (see Section 5).

Table 9 shows that, using 4 years of measurements done at the TMT potential sites during the site testing campaign and more than 14 years of observations done at the location of the Telescopio Nazionale Galileo (TNG, located near the summit of the Roque de los Muchachos), the median dust mass concentration at the ORM site is comparable to that of Maunakea, and both places rank significantly better than Armazones. Still, as expected, the distribution of the dust mass concentration is different between sites.

From a technical and science operational point of view, it is extremely important to maintain good optics reflectivity. Measuring dust concentration levels is thus paramount to determine when telescopes can operate without compromising science and telescope optics quality. Typically, ORM operators start monitoring closely the changes in the dust level at lower concentrations of 15 $\mu g/m^3$. Telescopes occasionally operate with mass concentration >50 $\mu g/m^3$, while a level of 100 $\mu g/m^3$ is the typical operational limits. From **Table 9**, we see that the fraction of time that mass concentration exceeds 15 $\mu g/m^3$ happens 11.5% of the time at ORM, while the same threshold is reached 6.8% and 5.4% of the time at MK13N and Armazones respectively. A level of 50 $\mu g/m^3$ is reached 2.3% of the time (this is about 8 days in a year, but mainly in summer months and consisting of a couple of large "Calima" events lasting several days each), while for Maunakea, the corresponding fraction of time is 3.6%. A mass concentration of 100 $\mu g/m^3$ or higher, when

ORM observatories must shut down operations happens about 0.5% of the time, or 2 nights per year on average, while the same threshold is reached 2.4% of the time at MK13N.

Table 9: Mass distribution of the dust density at MKO and ORM: Mass concentrations ≥15 μg/m^3 trigger a close operational monitoring while 100 μg/m^3 is the GTC operational limit (telescope enclosure is closed). Data for Armazones, San Pedro Martir Observatory and Cerro Tolonchar are shown for comparison.

Site	Median (μg/m^3)	Fraction of time exceeding		
		≥15 μg/m^3	≥50 μg/m^3	≥100 μg/m^3
ORM	1.006	11.5%	2.3%	0.54%
MK13N	0.815	6.8%	3.6%	2.40%
Armazones	2.290	5.4%	0.4%	0.32%
SPM	7.02	26.8%	13.9%	4.4%
Tolonchar	6.30	24.7%	8.9%	2.1%

The median surface dust mass concentration at ORM is about 1 μg/m^3 and the GTC team[3] has measured an extinction increase of about 0.1 mag/airmass (in V spectral band) for each additional 10 μg/m^3 of surface dust mass concentration. As a result, the dust mass concentration threshold of 15 μg/m^3 corresponds to a factor 15 increase in background mass dust concentration in comparison to the median value, leading to an increase of 0.15 mag in the V spectral band atmospheric extinction. To put this in context, thin cirrus clouds contribute to transparency variations of the order of 10% to 20% (i.e. 0.1 to 0.2 mag) (Kerber et al., 2016, Otarola & Hickson, 2017). As stated above, the average extinction for usable nights, regardless of cause, are equivalent to those of MK13N. In terms of operational efficiency and decrease of transparency, dust events have the same impact as thin cirrus.

Note: "Calima" events happen when strong convective dust events originating in the Saharan desert inject dust into the upper troposphere, which get advected into the Canary Islands by upper-level easterly winds. The amount of atmospheric extinction depends on the thickness and height above the site affected by advection of dusty air. "Calima" events at ORM are not as frequent as commonly believed in the context of a whole year of operations. The Carlsberg Meridian Telescope (CMT) conducted atmospheric extinction measurements for more than 30 years, and found that under all conditions (cloudy nights, wind, dust events, etc.), the downtime for the CMT was 20.7% (see Garcia-Gil et al., 2010). In other words, the available nights fraction for the CMT reached up to 79.3%. For TMT purposes, using all sources of information we have estimated a usable time fraction in the range 72% -74% (Otarola & Hickson, 2017).

1.2.5. IMPACT ON SCIENCE – SUMMARY

We used the measured characteristics of ORM to assess the ability of the site to support the large range of TMT science cases. All TMT science programs can be carried out from ORM, however

[3] Based on surface aerosols measurements and zero points on the GTC's OSIRIS instrument.

increased exposure times are needed to reach a S/N equivalent to observations made at a higher site like MK13N. **Table 10** shows the increase in exposure time required for programs at ORM in comparison to MK13N, as a function of the observing mode and wavelength regime. The most affected modes are imaging and low-resolution spectroscopy in Q band, which would require a considerable increase in exposure time. The estimates for the mid-infrared are valid for faint targets for which the target flux is small compared to the atmospheric flux (worst case scenario). For cases where the target flux is significant compared to the atmospheric radiance, the relative exposure time differences are reduced. Most programs would highly benefit from the use of adaptive scheduling in service mode, which would secure the most favorable atmospheric conditions for each program execution.

The average observing time increase for carrying out TMT science with its First-Light instruments (WFOS, IRIS, and MODHIS) is about 16%. If we consider all possible future instruments, including unplanned instruments that would sample the challenging mid-IR Q band (17-25 µm), the average increase in observing time across all wavebands and observing modes is estimated to be approximately 19% in comparison to MKO. More information on the details of these estimates can be found in Section 6.

Table 10: Expected increase of exposure time to carry out various observing programs at ORM in comparison to MK13N. Note that the exact values shown here depend on the specific assumptions made about targets and observation modes, and may vary somewhat when these assumptions are changed. They should, however, be generally representative of typical thermal/mid-IR observations.

	Observation type		Expected fraction of observing time		Increase in exposure time at ORM	Level of mitigation with adaptive queue
First-generation instrument	Optical		40%		2-3% median conditions	None
	Near-IR (AO assisted, λ< 2.5µm)	J imaging & spectr.	50%		23% median conditions	Moderate improvement
		H imaging & spectr.			20% median conditions	
		K imaging & spectr.			36% median conditions	
Second generation instrument	Mid-IR (AO assisted, λ=2.5-28µm)	L imaging (3.4-4.1µm)	10%	0.75%	68% (25% best conditions)	Significant improvement
		M imaging (4.55-4.8µm)		0.25%	97% (25% best conditions)	
		N imaging (8-12.5µm)		1.00%	30% (25% best conditions)	
		Q imaging (17-25µm)		0.25%	230% (25% best conditions)	
		L low-res spectr. (3.4-3.77µm)		1.00%	48% (25% best conditions)	
		M low-res spectr. (4.6-4.79µm)		0.25%	84% (25% best conditions)	
		N low-res spectr. (11-12µm)		1.00%	26% (25% best conditions)	
		Q low-res spectr. (17-19µm)		0.25%	150% (25% best conditions)	
		L high-res spectr.		1.75%	30% (25% best conditions)	
		M high-res spectr.		1.00%	63% (25% best conditions)	
		N high-res spectr.		2.00%	19% (25% best conditions)	
		Q high-res spectr.		0.50%	100% (25% best conditions)	

1.2.6. EFFECT OF CLIMATE CHANGE AND EXTREME WEATHER CONDITIONS

A study was performed, contracted by TMT, to evaluate the risks that climate change may significantly change the conditions for astronomy at any of the potential TMT sites. The study concentrated on investigating whether there is any evidence that the locations and sizes of the

atmospheric Hadley Cells are evolving over time. The report concluded that there are no long-term significant trends in PWV at any of the candidate sites, including Maunakea and La Palma.

Hawaii experiences a much higher frequency of cyclone weather systems comprising tropical depressions, storms, and hurricanes. Equivalent weather systems are almost non-existent in the area around the Canary Islands. **Figure 15** shows the tracks and intensity for all known tropical cyclones over the period 1947–2008. Note how Hawaii has been in the path of many systems whilst the Canary Islands rarely experiences effects from cyclones.

As described in Section 1.2.4, Calima events happen several times per year when Saharan dust is transported past the Canary Islands. In the majority of Calima events, the dust is constrained to the lower levels of the atmosphere, below the inversion layer though measurements show that, in a few cases, dust reaches the altitude of the observatories.

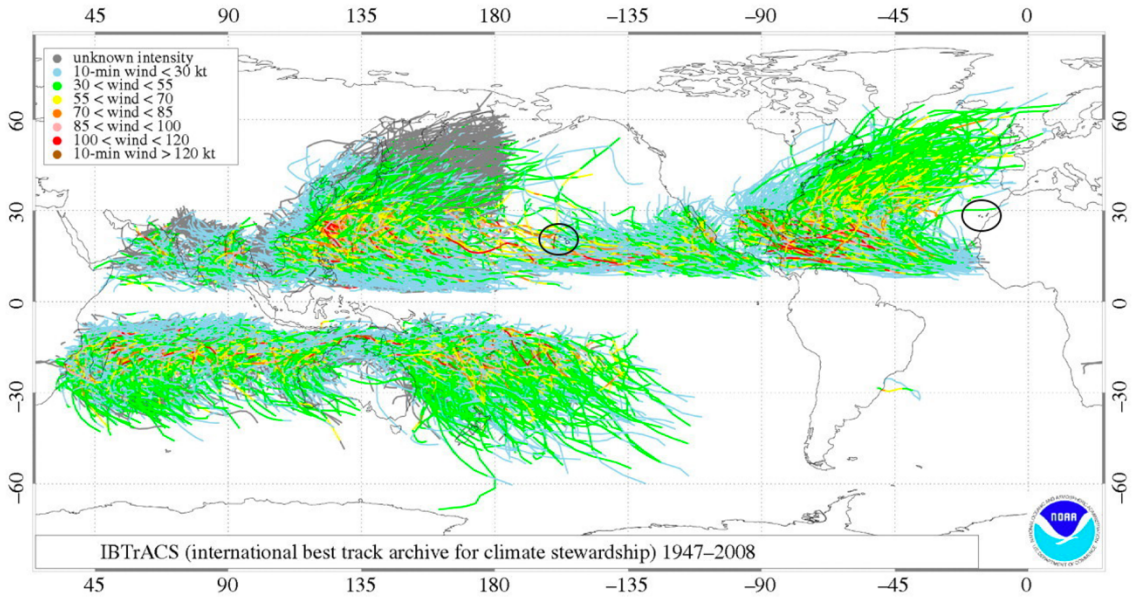

Figure 15: The above figure shows the observed tropical cyclone (tropical depressions, storms, and hurricanes) tracks and intensity for all known storms over the period 1947–2008. The locations of Hawaii and the Canary Islands are indicated (circled). While Hawaii is routinely impacted by tropical storms, La Palma is well protected from those. Overall, taking into account all unfavorable weather conditions, the percentage of usable time is the same at both sites.

2. CONCLUSION

Overall, all four alternate sites considered for TMT were excellent locations to host the telescope and could support all of TMT core science.

Roque de Los Muchachos Observatory is the lowest altitude site among all considered but it is the site that provides atmospheric characteristics at visible and near-IR wavelengths very similar to the properties measured for MKO. The main effect of the lower altitude and warmer temperature

of ORM would be to decrease slightly the efficiency of TMT science operations but ORM can support all TMT core-science goals.

Adaptive scheduling will be fully implemented as part of TMT's science operations and will have the net effect to boost science operations efficiency by ensuring execution of the most demanding scientific observations when the weather conditions best match those needed by these programs.

3. REFERENCES

- Bardou et al. 2018, "Error breakdown of ELT-elongated LGS wavefront-sensing using CANARY on-sky measurements", Proceedings of the SPIE, Volume 10703

- Benn et al. 2008, "GLAS/NAOMI: ground-layer AO at the William Herschel Telescope". Proceedings of the SPIE, Volume 7015

- Carrasco, Erasmus, Djorgovski, Walker and Blum, 2017, PASP 129:035005

- Castro-Almazán et al., 2018, PASP, 130:115002

- ESO, "The E-ELT construction proposal" (https://www.eso.org/public/archives/books/pdf/book_0046.pdf)

- Hermann, et al., Proc. 30th Int. Cosm. Ray Conf., R. Caballero et al. (eds.), UNAM, Mexico City, 2008, Vol. 3, pg. 1313-1316

- Herriot, Andersen, Atwood, Boyer, Beauvillier, Byrnes, Conan, Ellerbroek, Fitzsimmons, Gilles, Hickson, Hill, Jackson, Lardière, Pazder, Pfrommer, Reshetov, Roberts, Véran, Wang and Wevers, "NFIRAOS: TMT's facility adaptive optics system," 2010, Proc. SPIE, 7736, 77360B

- Kerber, Querel, Neureiter and Hanuschik, "Through thick and thin: Quantitative classification of photometric observing conditions on Paranal," Proc. SPIE 9910 (2016)

- Martin et al., 2014, "Detailed analysis of the Canary on-sky results at the WHT using Rayleigh laser guide stars", Proceedings of the SPIE, Volume 9148

- Myers et al., 2003, "NAOMI adaptive optics system for the 4.2m William Herschel telescope". Proceedings of the SPIE, Volume 4839, p. 647-658

- Otarola and Hickson, AO4ELT5 Conference Proceedings, Tenerife, Canary Islands, Spain, June 25-30, 2017

- Patat F. et al., 2011, A&A, 527, A91

- Ragazzoni et al. 2000a, "Adaptive-optics corrections available for the whole sky". Nature, vol 403, Issue 6765, pp. 54-56

- Ragazzoni et al., 2000b, "Testing the pyramid wavefront sensor on the sky", Proceedings of the SPIE, Volume 4007, p. 423-430

- Schöck et al., 2011, RevMexAA (Serie de Conferencias), 41, 32-35

- Schöck et al., 2009, PASP 121:384-395

- Schärmer et al., 2019, “Performance of the revamped Swedish 1-m Solar Telescope and its blue- and red-beam re-imaging systems”, A&A 626, A55.

- Sitarski et al., 2019, AO4ELT6 Conference Proceedings, Québec. City, Canada, June 9-14.

- Talbot et al., GLAS: engineering a common-user Rayleigh laser guide star for adaptive optics on the William Herschel Telescope, 2006, Proc. SPIE 6272, Advances in Adaptive Optics II, 62722H

- TMT-MIRSA, 2021, “TMT Mid Infrared Sensitivity Analysis”, available at https://www.tmt.org/page/site

- Travouillon, in Proc. SPIE 6267, 2006, Ground-based and Airborne Telescopes, ed. Stepp, L. M., 65

- Vogiatzis, Das, Angeli, Bigelow and Burgett, Computational Fluid Dynamics Modeling of GMT, SPIE 10705-28, Austin TX, June 10-15, 2018.

- Wang and Ellerbroek "Computer simulations and real-time control of ELT AO systems using graphical processing units,” 2012, SPIE 844723

4. ANNEX I (SELECTED PUBLISHED ORM SITE CHARACTERIZATION STUDIES)

- Bounhir, Benkhaldoun, Carrasco and Sarazin, "High-altitude wind velocity at Oukaimeden observatory", 2009, Monthly Notices of the Royal Astronomical Society, Volume 398, pp. 862-872

- Castro-Almazán and Muñoz-Tuñón "Climatological Study for the Cherenkov Telescope Array North Site at the Canary Islands I: Temperature, Precipitation, and Relative Humidity", November 2018, Publications of the Astronomical Society of the Pacific, Volume 130, Issue 993, pp. 115002

- Castro-Almazán, Muñoz-Tuñón, García-Lorenzo, Pérez-Jordán, Varela, Romero and Ignacio, "Precipitable Water Vapour at the Canarian Observatories (Teide and Roque de los Muchachos) from routine GPS", July 2016, Proceedings of the SPIE, Volume 9910

- Chueca, García-Lorenzo, Muñoz-Tuñón and Fuensalida "Statistics and analysis of high-altitude wind above the Canary Islands observatories", April 2004, Monthly Notices of the Royal Astronomical Society, Volume 349, Issue 2, pp. 627-631.

- Eff-Darwich, García-Lorenzo, Bonatto, Hernández-Gutiérrez, Viñas, Rodriguez-Losada, Blanco and Muñoz-Tuñón "The Impact of Seismicity on High Angular Resolution Astronomy:. the Case of the Canary Islands", September 2009, Proceedings of the Astronomy Meets Meteorology, Proceedings of the Optical Turbulence Characterization for Astronomical Applications Sardinia, pp. 342-349

- García-Gil, Muñoz-Tuñón and Varela "Atmosphere Extinction at the ORM on La Palma: A 20 yr Statistical Database Gathered at the Carlsberg Meridian Telescope", September 2010, Publications of the Astronomical Society of the Pacific, Volume 122, Issue 895, pp. 1109

- García-Lorenzo, Eff-Darwich, Castro-Almazán, Pinilla-Alonso, Muñoz-Tuñón and Rodríguez-Espinosa "Infrared astronomical characteristics of the Roque de los Muchachos Observatory: precipitable water vapour statistics", July 2010, Monthly Notices of the Royal Astronomical Society, Volume 405, Issue 4, pp. 2683-2696

- García-Lorenzo, Castro-Almazán, Eff-Darwich, Muñoz-Tuñón, Pinilla-Alonso, Rodriguez-Espinosa, and Romero "Precipitable water vapour content above the Roque de los Muchachos Observatory from GPS estimations", September 2009, Proceedings of the SPIE, Volume 7475

- García-Lorenzo, Fuensalida, Muñoz-Tuñón and Mendizabal "Astronomical site ranking based on tropospheric wind statistics", January 2005, Monthly Notices of the Royal Astronomical Society, Volume 356, Issue 3, pp. 849-858.

- Garcia-Lorenzo, Fuensalida, Mendizabal, Munoz-Tunon and Varela "Climate diagnostic archives: an approach to ELT site selection", November 2004, Proceedings of the SPIE, Volume 5572, pp. 68-75

- Garcia-Lorenzo, Chueca, Munoz-Tunon, Fuensalida and Mendizabal "Detailed study of 200-mbar wind speed at the Canary Islands", July 2004, Proceedings of the SPIE, Volume 5382, pp. 668-675

- Giordano, Vernin, Vázquez Ramió, Muñoz-Tuñón, Varela and Trinquet "Atmospheric and seeing forecast: WRF model validation with in situ measurements at ORM", April 2013, Monthly Notices of the Royal Astronomical Society, Volume 430, Issue 4, p.3102-3111

- Montilla et al. "The Gran Telescopio Canarias laser guide star AO system: error budget and expected performance", 2018, Proceedings of the SPIE, Volume 10703

- Muñoz-Tuñón, Varela and Fuensalida "Recent results at the Canarian Observatories", October 2007, Workshop on Astronomical Site Evaluation, Revista Mexicana de Astronomía y Astrofísica (Serie de Conferencias) Vol. 31, pp. 106-112

- Muñoz-Tuñón, Sarazin and Vernin "Site Selection for the European ELT: working package included in the European FP6 ``ELT design study'' contract", October 2007, Workshop on Astronomical Site Evaluation, Revista Mexicana de Astronomía y Astrofísica (Serie de Conferencias) Vol. 31, pp. 1-9

- Munoz-Tunon, Vernin and Sarazin "Site selection for the European ELT", July 2004, Proceedings of the SPIE, Volume 5382, pp. 607-618

- Pérez-Jordán, Castro-Almazán and Muñoz-Tuñón "Precipitable water vapour forecasting: a tool for optimizing IR observations at Roque de los Muchachos Observatory", July 2018, Monthly Notices of the Royal Astronomical Society, Volume 477, Issue 4, p.5477-5485

- García-Talavera et al. "GTC adaptive optics first performance tests in laboratory", 2018, Proceedings of the SPIE, Volume 10703

- Sicard et al., "Results of site testing using an aerosol, backscatter lidar at the Roque de los Muchachos Observatory", June 2010, Monthly Notices of the Royal Astronomical Society, Volume 405, Issue 1, pp. 129-142

- Sicard, Tomás, Reba, Comerón, Batet, Muñoz-Porcar, Rodriguez, Rocadenbosch, Muñoz-Tunon and Fuensalida "Aerosol stratification characterization of an astronomical site by means of a backscatter lidar at the Roque de los Muchachos Observatory", September 2009, Proceedings of the SPIE, Volume 7475

- Varela and Muñoz-Tuñón "Climatology at the Roque de LOS Muchachos Observatory", September 2009, Proceedings of the Astronomy Meets Meteorology, Proceedings of the Optical Turbulence Characterization for Astronomical Applications Sardinia, pp. 256-263

- Varela, Bertolin, Muñoz-Tuñón, Ortolani and Fuensalida, "Astronomical site selection: on the use of satellite data for aerosol content monitoring", December 2008, Monthly Notices of the Royal Astronomical Society, Volume 391, Issue 2, pp. 507-520.

- Varela, Bertolin, Muñoz-Tuñón, Fuensalida and Ortolani "Use of satellite data for astronomical site characterization", October 2007, Proceedings of the SPIE, Volume 6745, article id. 674508

- Varela, Bertolin, Muñoz-Tuñón, Fuensalida and Ortolani "In situ calibration using satellite data results", October 2007, Workshop on Astronomical Site Evaluation, Revista Mexicana de Astronomía y Astrofísica (Serie de Conferencias) Vol. 31, pp. 106-112

- Varela, Muñoz-Tuñón, García-Lorenzo and Fuensalida "Tropospheric wind regimes and site topographical effects: importance for site characterization", June 2006, Proceedings of the SPIE, Volume 6267

- Varela, Fuensalida, Muñoz-Tuñón, Rodríguez Espinosa, García-Lorenzo and Cuevas "Comparison of the aerosol index from satellites and the atmospheric extinction coefficient

above the Canarian Observatories", October 2004, Proceedings of the SPIE, Volume 5489, pp. 245-255

- Vázquez Ramió et al. "European Extremely Large Telescope Site Characterization. II. High Angular Resolution Parameters", August 2012, Publications of the Astronomical Society of the Pacific, Volume 124, Issue 918, pp. 868

- Vernin et al. "European Extremely Large Telescope Site Characterization I: Overview", November 2011, Publications of the Astronomical Society of the Pacific, Volume 123, Issue 909, pp. 1334

- Vernin, Muñoz-Tuñon and Sarazin E-ELT site characterization status", July 2008, Proceedings of the SPIE, Volume 7012, article id. 70121T, 12 pp.

5. ANNEX II (ADDITIONAL NOTES ON DUST CHARACTERIZATION AT ORM)

5.1. OPERATIONAL EXPERIENCE FROM EXISTING FACILITIES AT ORM

The GranTeCan (GTC) and Liverpool telescopes stop scientific operations when ground-level dust reaches the threshold of 100 µg/m^3. **Table 9** shows that this occurs <1% of the time at ORM.

For any event with dust levels below 20 µg/m^3, GTC staff does not notice any reduction in reflectivity above the standard slow degradation rates and routine monthly cleaning keeps the impact of ≤20 µg/m^3 events below a level that can be noticed. For events with concentration ≥20 µg/m^3 it is necessary to clean optics within one week to re-establish full reflectivity of the optics.

5.2. MIRROR DEGRADATION RELATIVE TO OTHER SITES

During development of the Gemini mirror coating, tests were carried out to compare the relative rates of degradation of bare aluminum versus protected silver (the baseline coating for TMT) at the Cerro Pachon site. The Gemini experiments found an aluminum degradation rate of ~11%/year, or 0.03%/day. After washing the reflectance returned to 0.2% of the freshly coated value[4]. The same testing for protected sliver found a degradation rate of 0.06%/day and a

[4] http://www.gemini.edu/media/pr_images/websplash2004-12/paper_SPIE04.pdf

restoration of full reflectivity after washing. Thus the degradation rates of bare aluminum and protected silver with CO_2 cleanings can be expected to be similar.

The Cherenkhov Telescope Array project carried out site testing at SPM, Armazones and Teide Observatories (Teide Obs. is located on the island of Tenerife, East of La Palma) and these test reports were provided to the TMT site testing group. The test mirrors were all aluminum with Al:SiO_2:HfO_2:SiO_2 layers, exposed continuously to ambient conditions with no protection and reflectivity measured using the same method. Because of the systematic nature of the testing, site-to-site differences are valid.

The effects of dust accumulation and mirror coating degradation after cleaning show that, among the alternate sites considered for TMT, Armazones is most impacted by dust, with twice the effects seen for Teide Obs.

A conservative conclusion is that dust accumulation and mirror degradation at ORM will not be worse than experienced at other observatory sites.

5.3. The Carlsberg Meridian Telescope (CMT) Extinction Measurements

The CMT gathered nightly means of the V-band extinction per unit airmass for over 30 years (this data set is widely available and described elsewhere[5]). **Table 11** shows the V-band extinction according to its probability distribution. The median extinction is very stable during the year, with a slight increase in the mean extinction in July and August (see **Figure 16**).

Table 11: Statistics of the 30 year nightly average CMT extinction measurements. The increased extinction due to the 1991 Mount Pinatubo eruption has been excluded.

Percentile	V band extinction (mag/airmass)
1%	0.096
5%	0.106
10%	0.110
25%	0.120
50%	0.132
75%	0.161
90%	0.270
95%	0.370
99%	0.624

[5] Garcia-Gil, A., et al., 2010, PASP, 122, 895

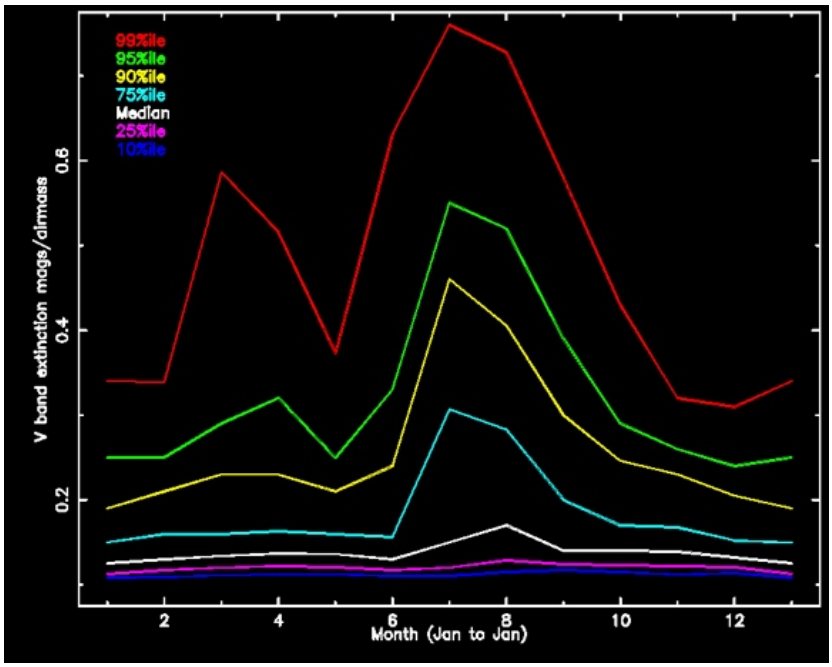

Figure 16: Monthly V band extinction statistics calculated using the full 30 year data set of CMT measurements, including higher extinctions for 3 years following the 1991 Mount Pinatubo eruption. The median extinction is very stable, the largest departure being in July and August, at the same time of year as the temperature and PWV summer variations as seen in **Figure 6**.

6. ANNEX III (NOTES ON ESTIMATING THE EXPOSURE TIME INCREASE FOR ORM - IN COMPARISON TO MK13N)

In **section 1.2.5**, we have listed the expected increase of exposure time to be applied at ORM in comparison to MK13N, as a function of the wavelength regime and observing mode (**Table 10**).

In this annex, we describe how the relative exposure time estimates were derived for each observing mode, and the reasons for differences from the estimates implied by the Site Merit Function (**section 1.1.5**,**Table 7**). Indeed, the Site Merit Function best relates to "classically scheduled" background limited observations that are dependent on the full statistical distributions of site characteristics.

Optical regime:

2-3% median conditions

This increase was simply derived using the relative median V-band transmission at the two sites, ORM/MK13N. Effects of seeing were not included. This estimation is valid for observations of sources that are not background limited.

1) The V-band extinction at ORM of 0.132 mags/airmass is derived from the Carlsberg Meridian Telescope (CMT) measurements (omitting increased extinction for a period following the Mount Pinatubo eruption).
2) The V-band extinction at MK of 0.111 mags/airmass for 550nm is listed in the Sky Transparency/Extinction information on the Keck website[6].
3) The relative transmission: $R = 10^{(0.132-0.111)/2.5} = 1.02$ corresponds to a 2% increase.

Because there is a small range of extinction values for each site from different data sets, the range 2% to 3% increase is quoted to be conservative.

Note that this estimate does not include a contribution from programs conducted at wavelengths around 340nm and shorter, because technical limitations of mirror coatings has a much larger effect than atmospheric transmission.

Also, the optical site merit function depends only on the seeing statistics and does not include extinction (effectively assuming that it is equal at all sites). The Site Merit Function is most appropriate for background limited observations of point sources.

Near-IR regime:

The ratios of the exposure times for MK13N and ORM were estimated from the right graph of **Figure 9**. These ratio curves were calculated using full models of AO performance for the turbulence profiles and the sky backgrounds at each site. The on-axis relative performance is most appropriate for IRIS IFU observations and the central several arc seconds of the IRIS imager.

Mid-IR regime:

The mid-IR Site Merit Function (**Table 7**) implies much longer exposure times needed to complete mid-IR science programs than those shown in **Table 10**.

There are 3 main reasons for this difference:

1) There are slightly different assumptions in the mid-IR SMF and in **Table 10** of the amount of time spent in each mode of mid-IR observation. The total amount of time assumed for mid-IR observations is 10% in both the table and the mid-IR SMF.
2)
    a. The SMF uses empirical functions with the PWV (fraction of time <2mm), median pressure and temperature as variables and applies powers to the variables that are based on the expected effect of each variable. Whereas, the values of relative exposure time in **Table 10** for mid-IR imaging and low resolution spectroscopy modes are based on models of the mid-IR performance also presented in **Figure 13**.
    b. The values in **Table 10** for mid-IR high resolution spectroscopy are based on the same telluric emission models used for the mid-IR performance models (see

[6] https://www2.keck.hawaii.edu/inst/common/exts.html

Section 1.2.2). Several challenging mid-IR high resolution spectroscopy observing programs were examined. In all cases the wavelength region(s) for the program were found to be regions with gaps between telluric lines that were large compared to the widths of the telluric lines and large compared to any doppler shift of astrophysical features being investigated (e.g. orbital doppler signature from exoplanets and doppler shifted spectral signature in solar system gas giant planets). The effect of pressure broadening on the narrow telluric lines (28% wider telluric lines at ORM than MK13N[7]) bounding each large gap was therefore minimal compared to the size of the gaps between the telluric lines and did not affect the programs considered. The relative emission backgrounds within the gaps between telluric lines was taken from plots of the emission models for 25th percentile PWV and temperature conditions and used to calculate the required increase in exposure time to reach the same signal to noise ratio.

3) The mid-IR SMF assumes no adaptive queue, programs would be conducted randomly (such as in a classically scheduled scenario) and exposure times would be affected based on the conditions at the time. The estimates in **Table 10** use the predicted backgrounds at MK and ORM as mentioned above in 2) for the 25th percentile conditions. Because of adaptive queue scheduling, mid-IR observations could be conducted in the optimum 10% of time, achieving better performance than the 25th percentile conditions. Thus, the relative increase in time to conduct programs at ORM represents a conservative estimate.

[7] linewdith = aL *(P-Pgas)/Po + aLself*Pgas/Po)*(Tref/T)^(1/2) ~ P/T^(1/2)